
follow this link for up to date mind map

UNIVERSITY OF HAMBURG

MASTER'S THESIS

**Automated Analysis of Meso-Scale
Ocean-Eddies from Model Data**

Author:
NIKOLAUS KOOPMANN

Supervisor:
PROF. DR. CARSTEN EDEN

October 29, 2014

Abstract

will be added last...

abstract

Contents

Legend	v
1 Introduction	1
1.1 Theory	1
1.1.1 Detection methods	1
1.1.2 Eddy Drift Speeds	2
1.1.3 The Integral Length Scale of Turbulence	4
1.2 Important Papers	4
1.2.1 ?	4
1.2.2 ?	5
1.2.3 Early Altimeter Data	5
1.2.4 ???	5
1.3 Methods	6
1.3.1 Satellite vs Model Data	6
1.4 Goals	8
2 The Algorithm	11
2.1 Step S00: Prepare Data	11
2.1.1 S00: Set Up	11
2.1.2 S00: Parallel Part	11
2.2 Step S01: Find Contours	11
2.3 Step S01b: Find Mean Rossby Radii and Phase Speeds	12
2.4 Step S02: Calculate Geostrophic Parameters	12
2.5 Step S03: Filter Eddies	12
2.5.1 Reshape for Filtering	12
2.5.2 Correct out of Bounds Values	12
2.5.3 Descent/Ascend Water Column and Apply Checks	12
2.6 Step S04: Track Eddies	15
2.7 Step S05: Cross Reference Old to New Indices	15
2.8 Step S06: Make Maps of Mean Parameters	16
2.9 Example	16
2.9.1 Map Parameters	16
2.9.2 Other Parameters	16
2.9.3 Running the Code	17
3 Results	19
4 Discussion	21
Appendix A Turbulence Aspects	23
Appendix B Eddy Categories	27
Appendix C Further Papers	29
Appendix D Derivations	33
Appendix E Preview...	39

Legend

Definition 1: Reynolds Number $\text{Re} []$	Definition 9: Kinetic Energy per mass $E_k [m^2/s^2]$	Definition 17: Brunt Väisälä frequency $N [1/s]$
Compares advection of momentum to frictional acceleration. $\text{Re} = \frac{UL}{\nu}$		$N^2 = g/\rho_0 \frac{\partial \rho}{\partial z}$
Definition 2: Rossby Number $\text{Ro} []$	Definition 10: Mechanical Energy per mass $E_k [m^2/s^2]$	Definition 18: Mean Layer thickness $H [m]$
Compares advection of momentum to Coriolis acceleration. $\text{Ro} = \frac{U}{fL}$	Sum of kinetic and potential Energy.	
Definition 3: Rhines Number $R_\beta []$	Definition 11: Rossby Radius $L_R [m]$	Definition 19: Layer Thickness/physical height of an isopycnal surface $h(x, y, t) [m]/h(x, y, \rho, t) [m]$
Ratio of Rhines scale to horizontal scale. $R_\beta = \frac{U}{\beta L^2} = \frac{a}{L} \text{Ro}$	The geostrophic wavelength. $L_R = c/f$	$h = H + \eta$ (in the layered model)
Definition 4: Burger Number $Bu []$	Definition 12: Steering Level z_S	Definition 20: Planetary Vorticity $\Omega [1/s]$
Ratio of relative vorticity to stretching vorticity. $\sqrt{Bu} = \frac{NH}{fL} = \frac{L_R}{L}$	The critical depth where the real part of the Doppler shifted phase speed $c_S(z_S) = c(z) - u(z) = 0$ vanishes. I.e. the depth where the Doppler shift creates a standing wave, causing the disturbances to grow in place instead of spreading in space, analogous to a <i>supersonic bang</i> .	$\Omega = 4\pi/\text{day}_{fix\star}$
Definition 5: mass $m [kg]$	Definition 13: Rhines Scale $L_\beta [m]$	Definition 21: Latitude $\phi [\text{rad}]$
	Scale at which earth's sphericity becomes important. $L_\beta^2 = \frac{U}{\beta}$	
Definition 6: gravitational acceleration $g [m/s^2]$	Definition 14: Gravity Wave Phase Speed $c [m/s]$	Definition 22: Earth's Radius $a [m]$
Value of surface normal component of all body forces.	$c = \sqrt{g'H}$	
Definition 7: vorticity $\omega [1/s]$	Definition 15: Reduced Gravity $g'(x, y, z) [m/s^2]$	Definition 24: Change of Planetary Vorticity with Latitude $\beta [1/ms]$
	In the layered model $g' = g \frac{\delta \rho}{\rho_0} = N^2 h$	$\beta = \frac{\partial f}{\partial y} = \Omega/a \cos \phi$
Definition 8: Buoyancy Vector $\mathbf{B} [1/s^2]$	Definition 16: Surface/interface Displacement $\eta(x, y) [m]$	Definition 25: Okubo-Weiss Parameter $O_w [1/s^2]$
$\mathbf{B} = -\frac{\nabla \rho \times \nabla p}{\rho^2}$		$O_w = \text{divergence}^2 + \text{stretching}^2 + \text{shear}^2 - \text{vorticity}^2$. A negative value indicates vorticity dominated motion, whereas a positive value indicates deformation.

Definition 26: Sea Surface Height **SSH** [m]

Definition 27: Isoperimetric Quotient **IQ** []

$\text{IQ} = A/A_c = \frac{A}{\pi r_c^2} = \frac{4\pi A}{U^2} \leq 1$.
The ratio of a ring's area to the area of a circle with equal circumference.

Chapter 1

Introduction

1.1 Theory

1.1.0.0.1 This chapter discusses the theory of meso-scale turbulence and parametrizations thereof. Geostrophic turbulence is typically characterized by rather stable, circular, coherent pressure anomalies, that rotate fluid around in a vortex in quasi-geostrophic equilibrium. These entities can persist for long periods of time in which they often travel distances on the order of hundreds of kilometers zonally. The fact that baroclinic instability forms these vortices instead of leading to a cascade to ever smaller scales ,as would be expected from chaotic turbulence, is a direct consequence of the inverse energy cascade of 2-dimensional motion. For a discussion of this phenomenon see appendix A. The atmospheric analog are storms and high-pressure systems, yet with much less difference between high- and low-pressure systems due to a smaller centrifugal force i.e. smaller Rossby number. These quasi-geostrophic, meso-scale vortices, from here on called eddies ¹, are immediately visible on SSH maps. Yet, it is difficult to physically *define* an eddy in terms of oceanographic variables. The transition from meandering jets or other undeveloped baroclinic turbulence is not very sharp. Eddies also sometimes merge or split or collectively form rifts and valleys in SSH. detecting them on one snapshot automatically via an algorithm is therefore not trivial. Further problems arise when the algorithm is also supposed to track them. Their shear abundance at any given time inevitably creates ambiguities between time steps. It is therefore necessary to set up a clear, unambiguous, sufficient (in the mathematical sense) definition.

1.1.1 Detection methods

- One way to find an eddy in SSH-data is to simply scan for closed contours at different values for z and then subject found entity to a series of necessary tests. Only if all criteria are met is an eddy found. This method was first used by ? and turned out to be the simplest yet most effective method, at least for satellite SSH data. Therefore, as a starting point, this method will be adopted and should also serve as a general definition of what will be referred to as an *eddy* hereafter².
? set the following threshold criteria for his algorithm:
 1. The SSH values of all of the pixels are above (below) a given SSH threshold for anticyclonic (cyclonic) eddies.
 2. There are at least $[threshold]$ pixels and fewer than $[threshold]$ pixels comprising the connected region.

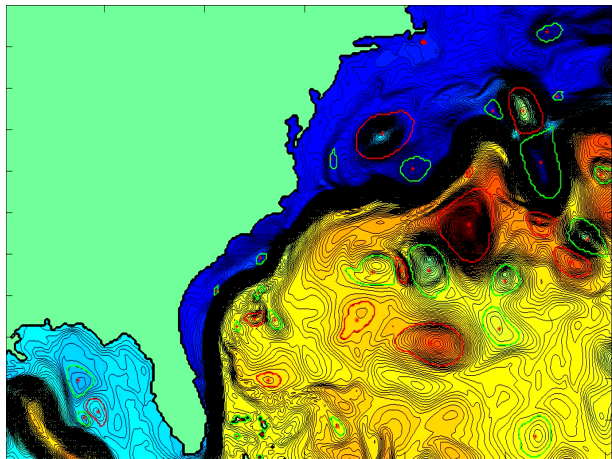


Figure 1.1: Animation snapshot of early test run. Shown is SSH with detected eddies indicated.

¹For a discussion of the different types of vortices in the ocean see appendix B
²The vortices will have names deviant from *eddy* where these criteria are altered.

3. There is at least one local maximum (minimum) of SSH for anticyclonic (cyclonic) eddies.
 4. The amplitude of the eddy is at least [threshold].
 5. The distance between any pair of points within the connected region must be less than [threshold].
- Another frequently used method to define an eddy makes use of the strain tensor \mathbb{T}^3 . The trace of the strain tensor squared includes valuable information about the dynamics of the velocity field. Namely

$$2O_w = \text{Tr } \mathbb{T}^2 = \text{divergence}^2 + \text{stretching}^2 + \text{shear}^2 - \text{vorticity}^2 \quad (1.1)$$

which reduces to $O_w = (\partial_x u)^2 + 2\partial_y u \partial_x v$ in 2 dimensions. This is called the Okubo⁴-Weiss-Parameter. It is a useful tool to determine whether the field has parabolic, vorticity dominated character, or whether deformation dominates giving hyperbolic character. An area of large negative values indicates high enstrophy density compared to gradients of kinetic energy, thus indicating little friction paired with high momentum i.e. a coherent, angular-momentum-conserving entity. Positive values on the other hand indicate incoherent deformation.

As genius as this parameter seems, it turns out that using it to identify eddies is often not the best solution. ? names 3 major drawbacks:

- No single threshold value for O_w is optimal for the entire World Ocean. Setting the threshold too high can result in failure to identify small eddies, while a threshold that is too low can lead to a definition of eddies with unrealistically large areas that may encompass multiple vortices, sometimes with opposite polarities.
- O_w is highly susceptible to noise in the SSH field. Especially when velocities are calculated from geostrophy, the sea surface has effectively been differentiated twice and then squared, exacerbating small discontinuities in the data.
- The third problem with the W -based method is that the interiors of eddies defined by closed contours of W do not generally coincide with closed contours of SSH. The misregistration of the two fields is often quite substantial.

It is hence only logical to scan for closed contours of SSH directly (as was done so by ?).

- vector based detection etc

1.1.2 Eddy Drift Speeds

Intuitively any translative motion of a vortex should stem from an asymmetry of forces as in an imperfectly balanced gyroscope wobbling around and translating across the table. The main effects that cause a quasi-geostrophic ocean eddy to translate laterally can easily be explained heuristically.

Lateral Density Gradient Consider a mean layer-thickness gradient $\frac{\partial h}{\partial x} > 0$ somewhere in the high northern latitudes and a geostrophic, positive density anomaly within that layer. In other words a high-pressure vortex or an anti-cyclonic eddy with length scale $L \approx L_R$. Hence a vorticity budget dominated by advection of relative vorticity and vortex stretching. Consider a parcel of water adjacent to the eddy on its eastern flank. Due to the eddy's negative vorticity, the parcel will be advected west into shallower layer-thickness where it will be squeezed vertically and acquire negative relative vorticity via term C in equation (B.1c). Analogously a parcel of initially zero ω on the eddy's western flank will be transported east, stretched and thereby acquire positive relative vorticity. The result is that the eddy will be shoved south from both zonal flanks. Note that the rotational sense of the eddy is irrelevant here. The drift direction is dictated by the sign of f . Hence eddies in the northern hemisphere will be pushed along gradients with the shallower water always on their right and vice versa on the southern hemisphere.

Planetary Lift Assume now that βL be comparable or larger even than $f_0 - \omega$ from the previous example. Then, all fluid adjacent to the eddy on its northern and southern flanks will be transported meridionally, thereby be tilted with respect to Ω and hence acquire relative vorticity to compensate. All fluid transported north will balance the increase in planetary vorticity with a decrease in relative vorticity and vice versa for fluid transported south. This is again independent of the eddy's sense

³see Derivation 7

⁴?

and in this case also independent of hemisphere since $\frac{\partial f}{\partial y} = \beta > 0$ for all latitudes. The result is that small negative vortices to the northern and small positive vortices to the southern flank of eddies will push them west.

Eddy-Internal β -Effect In the later case clearly particles within the vortex undergo a change in planetary vorticity as well. Or from a different point of view, since $U \sim \nabla p/f$, and noting that the pressure gradient is the driving force here and hence fix at first approximation, particles drifting north will decelerate and those drifting south will accelerate. In order to maintain mass continuity, the center of volume will be shifted west for an anti-cyclone and east for a cyclone. Another way to look at it is to note that the only way for the discrepancy in Coriolis acceleration north and south, whilst maintaining constant eddy-relative particle speed, is to superimpose a zonal drift velocity so that net particle velocities achieve symmetric Coriolis acceleration.

1.1.3 The Integral Length Scale of Turbulence

1.1.3.0.2 This section is intended to shed light on the benefits of exact determinations of ocean-eddy-scales. That is, their horizontal extent i.e. their diameter or *wavelength*.

1.1.3.0.3 Just like the *eddy* itself, its scale is rather vague and difficult to define. What physical parameter defines the outer edge of a seamless, smooth vortex? If the eddy is detected as done by ?, i.e. closed contours of SSH the interior of which fulfilling certain criteria, the measured perimeter may jump considerably from one time step to the next. An incremental difference in the choice of z might translate to a perimeter outlining twice the difference in area, especially when SSH gradients are small. Another possibility is to define an amplitude first, then assume a certain shape e.g. Gaussian, and then infer the radius indirectly. The obvious problem with this approach would be to properly define the amplitude.

The most physically sound method would have to be one depending on the eddy's most defining physical variable, that is unambiguously determinable from SSH. The geostrophic velocities. ?, as with everything else, tried all methods but also conclude that the later is the most adequate one.⁵

ref to technical chapter

1.1.3.0.4 Construed as an integral length scale of turbulence i.e. as the distance at which the auto-correlation of particles reaches zero, the *eddy-scale* turns out to be of fundamental relevance for attempts to parametrize geostrophic turbulence. General circulation models ($\mathcal{O}(10^2)$ km) as they are used in e.g. climate forecasts are too coarse to resolve meso-scale ($\mathcal{O}(10^1)$ km) turbulence. Even if the Von-Neumann-condition were ignored and a refinement were desired horizontally only, a leap of one order of magnitude would cause an increase in calculation time of factor⁶ $x = 100$. The effects of the nonlinear terms therefore have to be somehow articulated in an integral sense for the large grid-boxes in the model. A common approach is to assume that *eddy kinetic energy* $\bar{u}'\bar{u}'$ and *eddy potential energy* $w'\rho'$, akin to diffusive processes⁷, are proportional to the gradient of \bar{u} respective \bar{b} (down-gradient-parametrization⁸) (?), which leads to the problem of finding expressions for the *turbulent diffusivities* i.e. the rate at which gradients are diffused by turbulence. This parameter is by no means constant, instead it can span several orders of magnitude, itself depending on the strength of turbulence-relevant gradients, and sometimes even assuming negative values (?). Precise knowledge of the integral length scale and the physics that set it is hence vital for attempts to analyze and set values for eddy diffusivities and turbulence parametrizations in general.

ingredient to parametrizations of turbulence in e.g. non-eddy-resolving climate models.

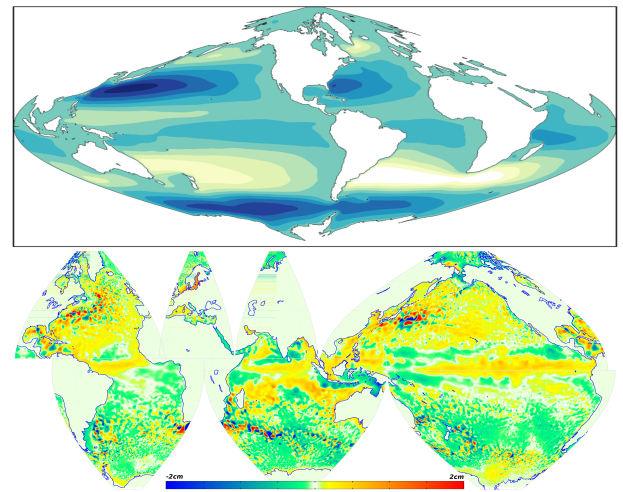


Figure 1.2: top: Stommel's equation $\mathcal{F}_{bottom} - \mathcal{F}_{surface} = -v\beta$ with constant eddy viscosity. bottom: Parallel Ocean Program eddy-resolving model snapshot with SSH mean of one year subtracted.

1.2 Important Papers

1.2.1 ?

Rhines investigated the effect of the β -plane on the inverse energy cascade of quasi-2-dimensional atmospheric and oceanic turbulence. At constant f , energy should be cascaded to ever-larger scales until halted by the scale of the domain. This is clearly not the case, as no storm has ever grown to global scale. The presence of a meridional restoring force creates a critical scale beyond which the *turbulent migration of the dominant scale nearly ceases* Instead, Rossby waves are excited which would theoretically eventually give way to alternating zonal jets of width L_β . This scale was later coined the Rhines Scale.

⁵See Chapter

⁶With the Moore's-Law-type exponential growth in FLOP/S of the last 22 years for supercomputers ($\lg(x) \sim 3/11a$) a factor 100 interestingly translates to only $a = 22/3 \approx 7$ years...

⁷In analogy to Fick's first law of diffusion

⁸i.e. Reynolds averaging

1.2.2 ?

? already noted that the β -effect causes a mass-imbalance in planetary vortices that, if not met by an asymmetry in shape must lead to westward propagation. ? derived that the β -effect results in a net meridional force on the integrated mass of the vortex, which in balance with the Coriolis acceleration shoves cyclones eastward and anti-cyclones westward. They also explained how displaced water outside the eddy's perimeter causes a much stronger westward component, with the result that all eddies propagate westward irrespective of rotational sense. The westward drift was also derived in various forms by e.g. ??.

? put it all into a less restricted uniform formalism by scaling the terms in the one-layer primitive equations by their respective dimensionless numbers. By integrating the interface-displacement caused by the eddy over the eddy's domain and applying mass continuity they derived for the location (X, Y) of an eddy's centroid⁹:

$$\begin{aligned}\Pi X_{tt} - Y_t &= \mathbf{L}_R T\beta \langle yv \rangle + L \frac{\beta}{f} \langle y\eta v \rangle \\ \Pi Y_{tt} - X_t &= -\mathbf{L}_R T\beta \langle yu \rangle - L \frac{\beta}{f} \langle y\eta u \rangle\end{aligned}\quad (1.2)$$

where $\Pi = 1/f_0 T$.

Hence, independent of balance of forces the eddy's center of mass describes inertial oscillations¹⁰ on the f -plane, even in the absence of β . Using geostrophic values for \mathbf{u} and returning to dimensional variables equation (1.2) can be cast into:

$$X_t = \frac{\omega_{long}}{k} \left(1 + \frac{1}{H} \frac{\int \eta^2 dA}{2V_e} \right) \quad (1.3)$$

The first term represents the **Planetary Lift** from 1.1.2, whereas the second term represents the **Eddy-Internal β -Effect**. Note that the first term is always westwards, while the second has sign of $-\eta$, i.e. westward for anti-cyclones and eastward for cyclones and that the first is always larger than the second.

for derivation
if time

1.2.3 Early Altimeter Data

The advent of satellite altimetry, which Walter Munk called *the most successful ocean experiment of all time* (?), finally allowed for global-scale experimental investigations of oceanic planetary phenomena on long time- and spatial scales. Among others, ??? were the first to use satellite-data to present evidence for the existence of Rossby waves and their westward-migration in accord with theory. Surprisingly all of the observations found the phase speeds to be 1 to 1.5 times larger than what theory predicted. Several theories to explain the discrepancy were presented. E.g. ? argued that the discrepancy was caused by mode-2-east-west-mean-flow velocities. Interestingly it appears that hitherto, the relevant altimeter signal was mainly associated with linear waves. Non-linearities are rarely mentioned in the papers of those years. Probably simply due to the fact that the turbulent character of much of the meso-scale variability was still obscured by the poor resolution of the first altimeter products.

1.2.4 ???

From the beginning of satellite altimetry ? have continuously invested tremendous effort to thoroughly analyze the data in terms of Rossby waves and geostrophic turbulence. At the time of their ? paper only 3 years of Topex/Poseidon data alone had been available, which led them to interpret the data mainly in terms of Rossby waves. Once the merged Aviso T/P and ERS 1/2 was released 7 years later, ? presented a new analysis that was based on an automated eddy-tracking algorithm using the geostrophic Okubo-Weiss parameter¹¹¹². For the first time Satellite data was sufficiently fine resolved to unveil the dominance of *blobby (sic) structures rather than latitudinally β -refracted continuous crests and troughs* that had hitherto been assumed to characterize the large scale SSH picture. They presented results of a refined algorithm in their ? paper, in which they abandoned the Okubo-Weiss concept and instead identified eddies via closed contours of SSH itself¹³. Among their most significant findings is the conclusion that on the one hand, the vast majority of extra-tropical west-ward propagating SSH-variability consists of

ref

⁹ $\langle \rangle \equiv \frac{1}{A} \int_A dA$

¹⁰compare to *harmonic oscillator*

¹¹see section 1.1.1

¹²see Derivation 7

¹³note that geostrophic O_w is a second derivative of SSH and thus exacerbates noise in the SSH data.

rephrase

coherent, isolated, non-linear, meso-scale eddies, whilst on the other hand, these eddies propagate about 25% slower¹⁴ than small amplitude features of larger lateral scale, that are difficult to separate from the data and are assumed to obey linear Rossby wave theory. Apart from this they find little evidence for any dispersion in the signal, neither do they find evidence for significant meridional propagation, as should be found for Rossby waves. In agreement with ?, they find this eddy-dominated regime to fade in vicinity of the equator, giving way to the characteristic Rossby-wave profile. Almost all of their eddies propagate westwards. Those that are advected eastwards by e.g. the ACC show significantly shorter life-times than those that are not. For more detail on their results and a discussion of the limitations of eddy-tracking via satellites see section ??.

1.3 Methods

1.3.1 Satellite vs Model Data

1.3.1.0.5 Satellites The latest Aviso SSH data from satellites features impressive accuracy, constancy and resolutions in both space and time. This is achieved by collecting all of the data from all of the altimeter-equipped satellites available at any given moment for any given coordinate. This conglomerate of highly inhomogeneous data is then subjected to state-of-the-art interpolation methods to produce a spatially and temporally coherent product. One satellite alone is not sufficient to adequately resolve meso-scale variability globally. Take e.g. the Topex/Poseidon satellite. It had a ground repeat track orbit of 10 days and circled the earth in 112 minutes or ≈ 13 times a day with a swath width of 5 km. Hence it drew ≈ 26 5 km-wide stripes onto the globe every day. This pattern is then repeated after 10 days, which means that at the equator only $10 \times 26 \times 5 = 1300$ km of the $2\pi \times 6371 = 40000$ km get covered, i.e. 3.25%. At every 10d time step, on average, effectively $40000/1300 - 5 = 20$ km are left blank in-between swaths on the equator. This is why, no matter how fine the resolution within the swath at one moment in time may be, the spatial resolution is so coarse.

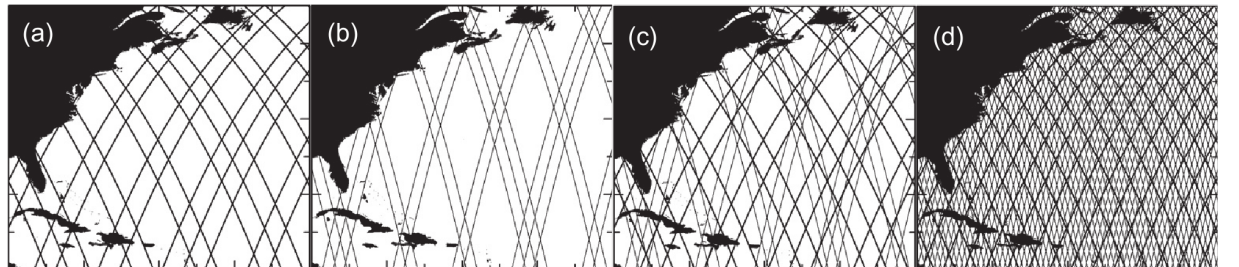
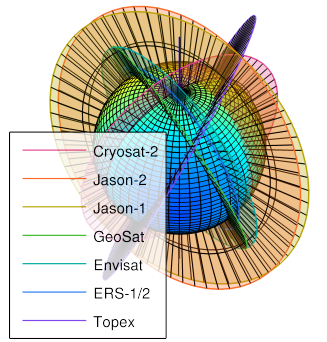


Figure 1.4: The ground track patterns for the 10-day repeat orbit of T/P and its successors Jason-1 and Jason-2 (thick lines) and the 35-day repeat orbit of ERS-1 and its successors ERS-2 and Envisat (thin lines). (a) The ground tracks of the 10-day orbit during a representative 7-day period; (b) The ground tracks of the 35-day orbit during the same representative 7-day period; (c) The combined ground tracks of the 10-day orbit and the 35-day orbit during the 7-day period; and (d) The combined ground tracks of the 10- day orbit and the 35-day orbit during the full 35 days of the 35-day orbit. (sic) ?

The merged ERS-1/Topex-data as used by ? has a time step of 7 days. Assuming eddy drift speeds of $u_e = \mathcal{O}(10^{-1})$ m/s implies a distance traveled per time step of $L_{\delta t} \approx 60$ km. ? estimate their effective spatial resolution as $\delta x \approx 40$ km. Eddies of smaller scale are not resolved. Tracking a single eddy from one time-step to the next should hence be feasible, especially when \mathbf{u}_e is approximately known. Problems arise when the sea level is characterized by an abundance of isolated vortices plus maybe even further meso-scale noise of comparable amplitude.

Ambiguities arise in terms of correctly matching the eddies from the old time-step with those in the new one, potentially causing aliasing effects in the final statistics. The translational speeds¹⁶ of eddies are not really the

¹⁴pointing to dispersion.

¹⁶ $\mathcal{O}(10^1)$ km/day

	POP	merged T/P - ERS-1 ¹⁵
dx	7km – 11km	1/3° ($\approx 40\text{km}$ after filtering)
dt	1d	7d
$\log_{10} 2$ filter cutoff	n/a	2° by 2°
z-levels	42	1
variables	SSH,S,T,u,v,w,tracers	SSH
pot. interpolation artifacts	n/a	yes
reality	no	yes

problem here, as they usually drift slow enough to not cover more than 1 grid node per 7 day time step. The issue are those areas where eddies are born, die and merge. According to ? instabilities within the ACC grow at rates of up to $1/(2\text{days})$, which means that at a time-step up to 3 eddies have emerged and equally many died for every eddy identified within such region. The ground-repeat frequency of a satellite can of course not be set arbitrarily. Especially when the satellite is desired to cover as far north and south as possible, whilst still being subjected to just the right torque from the earth's variable gravitational field to precess at preferably a sun-synchronous frequency i.e. $360^\circ/\text{year}$. Neither can the satellite's altitude be chosen arbitrarily. If too low the oblateness of the earth creates too much eccentricity in the orbit that can no longer be *frozen* ¹⁷. Another problem could be potential inhomogeneity in the merged data in time dimension, since products of old and current missions are lumped together into one product. This is why ? opted against the finest resolution available and instead went for a product that had the most satellites merged in unison for the longest period of time.

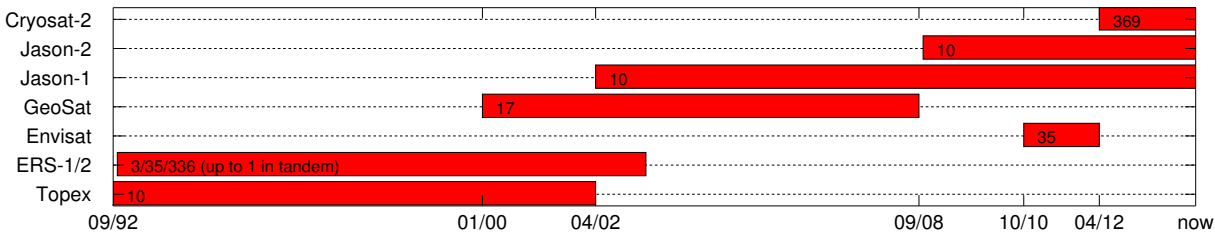


Figure 1.5: Length of mission. Numbers are orbit-period in days.

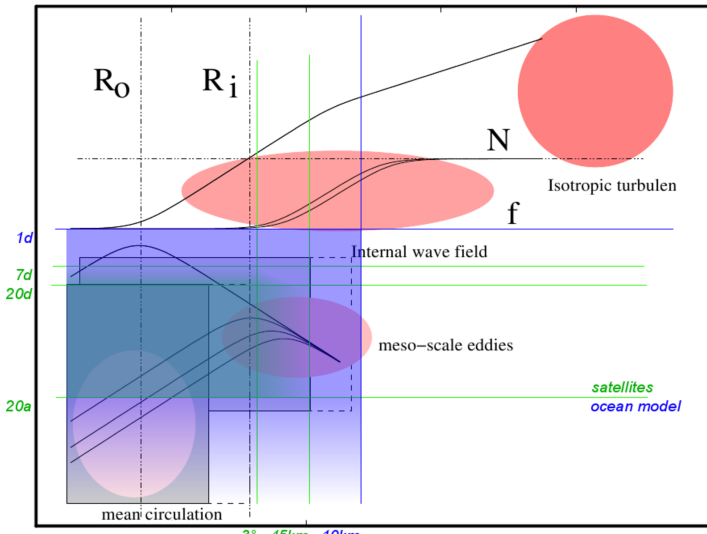


Figure 1.3: Resolutions for model vs satellite. Modified version from ?.

¹⁷minimizing undulating signals in altitude by choosing the right initial values.

1.3.1.0.6 Ocean Model The advantages of detecting and tracking eddies from model data are obvious. Say you have $Bu = 1$, so that $L = NH/f$. Let's assume ¹⁸ $NH = a/10d$, a model resolution of $1^\circ/\mu$ and that the eddy diameter was twice the Rossby radius. How many grid notes ξ fit into one eddy as a function of latitude?

$$\begin{aligned}\xi \frac{a \cos \phi}{\mu} &= \frac{2NH}{f} = \frac{2NH1d}{4\pi \sin(\phi)} \\ \xi &= \frac{2\mu}{10 \sin(2\phi)}\end{aligned}\quad (1.4)$$

See figure 1.6 for the results. In this flat-bottom, constant ρ_z , Mercator-gridded model the worst eddy-resolution is interestingly at mid-latitude. A value of $\xi > 2$ is desirable, because it eradicates ambiguities in the tracking procedure, with the result that there is no need to *forecast* the position x_e of an eddy for the new time step. It suffices to determine the closest eddy from the previous time-step for respective eddy from the new time step and vice versa. Those 2 eddies that are in agreement are successfully matched, those from the new (old) time step that do not find a match have just been born (have died). See also section for the technical stuff. Another major advantage of the model is that it produces not only SSH data but also all other relevant variables ¹⁹, for not only the surface but for many different depths. The surface velocities inferred from altimetry are the geostrophic components only, which should suffice to e.g. determine the non-linearity and kinetic energy of an eddy for almost all regions, but less so for e.g. the western boundary currents. The *one* draw-back of using model data is that, in contrast to the satellite data, it does not represent reality. ²⁰

ref to section

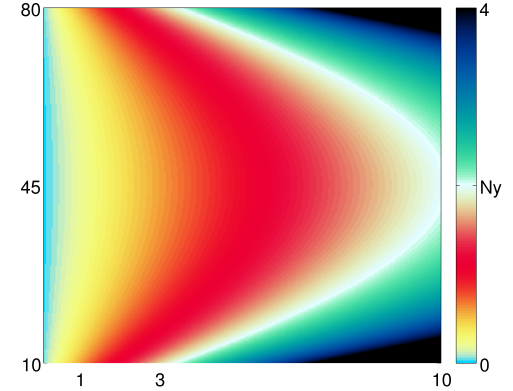


Figure 1.6: $\xi(\phi, \mu)$. $Ny \equiv 2$ i.e. the Nyquist frequency.

1.4 Goals

Not all of these will be achieved of course. They will be worked through in the order they appear until the time scope of this thesis is over.

1. Implement an efficient, parallelized, portable, modular algorithm entirely in matlab with focus on straightforwardness, easy maintainability and tweakability.
2. Mimic the algorithm as described by ? and apply it to the model data.
3. Repeat all of the analysis done by ? and compare.
4. Test alternative definition of the *center* of an eddy as the absolute value of the center of volume of the eddy measured from reference height (z of its perimeter).
5. Test alternative shape-threshold criterion based on isoperimetric coefficient i.e. the eddy's sphericity. ²¹
6. Compare theoretical phase and group velocities of Rossby waves at wavelength set to determined scale of eddies with eddy velocities.
7. Compare theoretical wave length of Rossby waves at phase/group speed set to determined drift speed of eddies with eddy scale, similar to (?).
8. Compare scales to those derived from linear stability analysis by e.g. ???.
9. Analyze eddy-genesis and fate. Look at mean values ²² Ro , Bu , R_β , track, scale, as a function of location.

¹⁸ corresponds to $L(\phi = 30^\circ) = 100\text{km}$

¹⁹ See section 1.4 for all the possibilities that arise.

²⁰ to be continued

²¹? guaranteed sphericity by demanding that *The distance between any pair of points within the connected region must be less than a specified maximum.*

²² either means in time or means in space.

10. Down-sample the model data, and compare runs for model/satellite at identical resolution and code.
11. Go sub-surface and apply the algorithm to at least one other depth than the surface, with the hypothesis that this might help to avoid meso-scale noise in highly turbulent locations.
12. Use findings from model to improve Aviso tracking.
13. Filter the SSH-data via Galilean-/LES-decomposition ? or simply by a filter created from determined mean shapes of eddies as a function of location. The motivation is again to successfully track eddies through zones of strong turbulence.
14. focus on regions of large Rossby number and regions of strong turbulence (ACC).
15. Calculate the *effective* Rossby radius as mentioned in ? and compare to eddy scales.
16. Include short lived eddies. ? only analyzed eddies with life times longer than 16 weeks in order to exclude less *robust* eddies for which they did not fully trust their algorithm to be capable of tracking correctly.
17. Test whether tracers inside eddy stay on isopycnals.
18. Determine tracks of tracers inside eddy and compare to the eddie's track.

Chapter 2

The Algorithm

This section walks through the algorithm step by step, so as to explain which methods are used and how they are implemented. The idea is that the code from step S01... on can only accept one well defined structure of data. In earlier versions the approach was to write code that would adapt to different types of data automatically. All of this extra adaptivity turned out to visually and structurally clog the code more than it did offer much of a benefit. The concept was therefor reversed. `S00_prep_data` can be altered to produce required output. Yet, there should be no need to adapt any of the later steps in any way. All input parameters are to be set in `input_vars.m`.

2.1 Step S00: Prepare Data

```
function S00_prep_data
```

Before the actual eddy detection and tracking is performed, SSH-, latitude- and longitude-data is extracted from the given data at desired geo-coordinate bounds and saved as structures in the form needed by the next step (S01).

2.1.1 S00: Set Up

```
function [DD]=set_up
```

The main purpose of this step is to Find the boundary-indices in the data describing a window that includes the user-chosen geo-coordinate window.

2.1.2 S00: Parallel Part

```
function spmd.body(DD)
```

This function distributes chunks of data (i.e. bins of files) to the threads, which then perform the cutting and save their outputs to `'../DATA/CUTS/'`. The code can handle geo-coordinate input that crosses the longitudinal seam of the input data. E.g. say the input data comes in matrices that start and end on some (not necessarily strictly meridional) line straight across the Pacific and it is the Pacific only that is to be analyzed for eddies, the output maps are stitched accordingly. If the desired range is zonally continuous e.g. the entire southern ocean, the first tenth (zonally) of the input data is appended to the end of the output. This ensures that eddies right on the seam can be found and that eddies can be tracked across the seam. This results in eddies being identified twice in `function S03_filter_eddies.m`. Such ref

2.2 Step S01: Find Contours

```
function S01_contours
```

The sole purpose of this step is to apply MATLAB's `contourc.m` function to the SSH data. It simply saves one file per time-step with all contour indices appended into one vector ¹. The contour intervals are determined by the user defined increment and range from the minimum- to the maximum of given SSH data.

The function `initialise.m`, which is called at the very beginning of every step, here has the purpose of rechecking the `cuts` for consistency and correcting the time-steps accordingly (i.e. when files are missing). `initialise.m` also distributes the files to the threads i.e. parallelization is in time dimension.

¹see the MATLAB documentation.

2.3 Step S01b: Find Mean Rossby Radii and Phase Speeds

```
function S01b_BruntVaisRossby
```

TODO!

2.4 Step S02: Calculate Geostrophic Parameters

```
function S02_infer_fields
```

This step reads the cut SSH data from `S00_prep_data` to

- use one of the files' geo-information to determine f , β , g and the ratio g/f .
- calculate geostrophic fields from SSH gradients.
- calculate deformation fields (vorticity, divergence, stretch and shear) via the fields supplied by the last step.
- calculate O_w .

2.5 Step S03: Filter Eddies

```
function S03_filter_eddies
```

Since indices of all possible contour lines at chosen levels are available at this point, it is now time to subject each and every contour to a myriad of tests to decide whether it qualifies as the outline of an eddy as defined by the user input threshold parameters.

2.5.1 Reshape for Filtering

```
function eddies2struct
```

In the first step the potential eddies are transformed to a more sensible format, that is, a structure `Eddies(EddyCount)` where `EddyCount` is the number of all contours. The struct has fields for level, number of vertices, exact i.e. interpolated coordinates and rounded integer coordinates.

2.5.2 Correct out of Bounds Values

```
function CleanEddies
```

The interpolation of `contourc.m` sometimes creates indices that are either smaller than 0.5 or larger than $N + 0.5$ ² for contours that lie along a boundary. After rounding, this seldomly leads to indices of either 0 or $N + 1$. These values get set to 1 and N respectively in this step.

2.5.3 Descent/Ascend Water Column and Apply Checks

The concept of this step is a direct adaption of the algorithm described by ?. It is split into two steps, one for anti-cyclones and one for cyclones. Consider e.g. the anti-cyclone situation. Since all geostrophic anti-cyclones are regions of relative high pressure, all anti-cyclones³ effect an elevated `SSH` i.e. a *hill*. The algorithm ascends the full range `SSH` levels where contours were found. Consider an approximately Gaussian shaped AC that has a peak `SSH` of say 5 increments larger than the average surrounding waters. As the algorithm approaches the sea surface from below, it will eventually run into contours that are closed onto themselves and that encompass the AC. At first these contours might be very large and encompass not only one but several ACs and likely also cyclones, but as the algorithm continues upwards found contour will get increasingly circular, describing some outer *edge* of the AC. Once the contour and its interior pass all of the tests the algorithm will decide that an AC was found and write it and all its parameters to disk. The AC's region i.e. the interior of the contour will be flagged from here on. Hence any inner contour further up the water column will not pass the tests. Once all AC's are found for a given time-step, the `SSH` flags get reset and the entire procedure is repeated only this time *descending* the `SSH`-range to find cyclones. The tests for cyclones and anti-cyclones are identical except for a factor -1 where applicable. In the following the most important steps of the analysis are outlined.

²where N as the domain size

³henceforth abbreviated AC

2.5.3.1 NaN-Check Contour

```
function CR.RimNan
```

The first and most efficient test is to check whether indices of the contour are already flagged. Contours within an already found eddy get thereby rejected immediately.

2.5.3.2 Closed Ring

```
function CR.ClosedRing
```

Contours that do not close onto themselves are obviously not eligible for further testing.

2.5.3.3 Sub-Window

```
function get_window_limits
function EddyCut_init
```

For further analysis a sub-domain around the eddy is cut out of the SSH data. These functions determine the indices of that window and subtract the resultant offset for the contour indices.

2.5.3.4 Logical Mask of Eddy Interior

```
function EddyCut_mask
```

Basically this function creates a [flood-fill](#) logical mask of the eddy-interior. This is by far the most calculation intensive part of the whole filtering procedure. A lot more time was wasted on attempting to solve this problem more efficiently than time could have been saved would said attempts have been successful. The current solution is basically just MATLAB's `imfill.m`, which was also used in the very first version of 09/2013.

2.5.3.5 Islands

```
function CR.Nan
```

No flags within the eddy are allowed. This check also avoids contours around islands as all land is flagged *a priori*.

2.5.3.6 Sense

```
function CR.sense
```

All of the interior SSH values must lie either above or below current contour level, depending on whether anti-cyclones or cyclones are sought.

2.5.3.7 Area

```
function EddyCircumference
```

Area described by the contour. This is needed for 2.5.3.9. This is not however related to the actual eddy scale determined in 2.5.3.12.

2.5.3.8 Circumference

```
function EddyCircumference
```

Line-length (sum of Euclidean norm of all nodes) of the contour.

2.5.3.9 Shape

```
function CR_Shape
```

This is the crucial part of deciding whether the object is *round enough*. A perfect vortex with $\frac{\partial u}{\partial y} = -\frac{\partial v}{\partial x}$ is necessarily a circle. The problem is that eddies get formed, die, merge, run into obstacles, get asymmetrically advected etc. To successfully track them it is therefore necessary to allow less circle-like shapes whilst still avoiding to e.g. count 2 semi merged eddies as one. This is achieved by calculating the **isoperimetric quotient**, defined as the ratio of a ring's area to the area of a circle with equal circumference. ? use a similar method. They require:

The distance between any pair of points within the connected region must be less than a specified maximum (?).

While this method clearly avoids overly elongated shapes it allows for stronger deformation within its distance bounds.

compare both,
show pictures

2.5.3.10 Amplitude

```
function CR_AmpPeak
```

This function determines the amplitude i.e. the maximum of the absolute difference between SSH and current contour level and the position thereof as well as the amplitude relative to the mean SSH value of the eddy interior as done by ?. The amplitude is then tested against the user-given threshold. The function also creates a matrix with current contour level shifted to zero and all values outside of the eddy set to zero as well.

2.5.3.11 Profiles

```
function EddyProfiles
```

This step saves the meridional and zonal profiles of SSH, U and V.

2.5.3.12 Dynamic Scale

```
function EddyRadiusFromUV
```

The contour line that is being used to detect the eddy is not necessarily a good measure of the eddy's *scale* i.e. it doesn't necessarily represent the eddy's outline very well. This becomes very obvious when the area, as inferred by 2.5.3.7, is plotted over time for an already successfully tracked eddy. The result is not a smooth curve at all. This is so because at different time steps the eddy usually gets detected at different contour levels. Since its surrounding continuously changes and since the eddy complies with the testing-criteria the better the closer the algorithm gets to the eddy's peak value, the determined area of the contour jumps considerably between time steps. This is especially so for large flat eddies with amplitudes on the order of 1cm. If the contour increment is on that scale as well, the difference in contour-area between two time steps easily surpasses 100% and more. Since there is no definition for the *edge* of an eddy, it is here defined as the ellipse resulting from the meridional and zonal diameters that are the distances between first minimum and maximum orbital velocity, away from the eddy's peak in positive and negative y and x directions respectively. In the case of a meandering jet with a maximum flow speed at its center, that is shedding off an eddy, this scale corresponds to half the distance between two opposing center-points of the meander. It is also the distance at which a change in vorticity polarity occurs and is thus assumed to be the most plausible *dividing line between vortices*. In practice the velocity-gradient profiles need to be smoothed to successfully

theres probably
a better way via
okubo weiss!

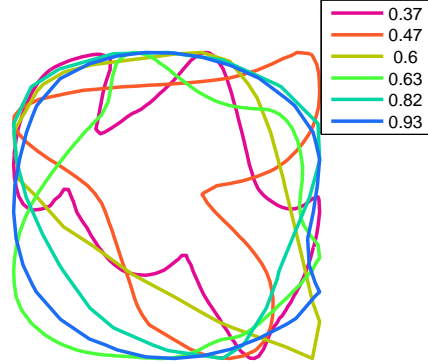


Figure 2.1: Different values of the isoperimetric quotient.

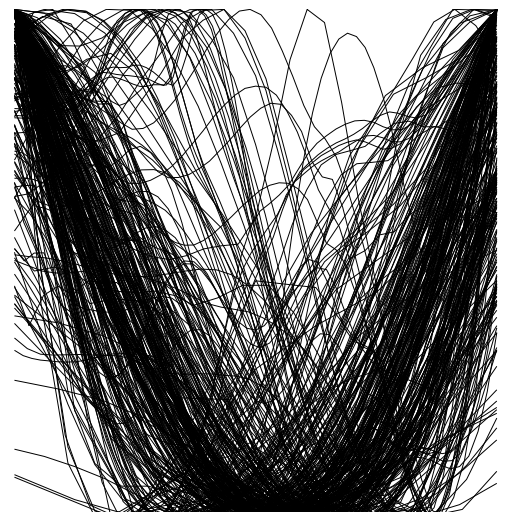


Figure 2.2: Zonal x- and z-normalized cyclone-profiles.

determine their first adequate zero-crossing. Once the zero crossings in all 4 directions are found, their mean is taken as the eddy's scale. Note that this is again similar to what ? did.

2.5.3.13 Dynamic Amplitude

```
function EddyAmp2Ellipse
```

As mentioned above, the contour that helps to detect the eddy is not representative of its extent. This is also true for the z -direction, for the same reasons. This function therefor takes an SSH-mean at indices of the ellipse created by the determined zonal and meridional *dynamical* diameters, and uses this as the basal value to determine a *dynamic* amplitude.

2.5.3.14 Center of Volume

```
function EddyArea2Ellipse
```

```
function CenterOfVolume
```

Instead of using the geo-position of the eddy's peak in the tracking procedure, it was decided to instead use the center of the volume created by the basal shifted matrix from 2.5.3.10 i.e. *the center of volume of the dome (resp. valley) created by capping off the eddy at the contour level*. This method was chosen because from looking at animations of the tracking procedure it became apparent that, still using peaks as reference points, the eddy sometimes jumped considerably from one time step to the next if two local maxima existed within the eddy. E.g. in one time-step local maximum A might be just a little bit larger than local maximum B and one time-step later a slight shift of mass pushes local maximum B in pole position, creating a substantial jump in the eddy-identifying geo-position hence complicating the tracking procedure.

2.6 Step S04: Track Eddies

```
function function S04_track_eddies
```

Due to the the relatively fine temporal resolution (daily) of the model data, the tracking procedure turns out to be much simpler than the one described by ?. There is really no need to project the new position of an eddy, as it generally does not travel further than its own scale in one day. This means that one eddy can be unambiguously tracked from one time step to the next as long both time-steps agree on which eddy from the other time-step is located the least distance away. The algorithm therefor simply builds an arc-length-distance matrix between all old and all new eddies and then determines the minima of that matrix in both directions i.e. one array for the new with respect to the old, and one for the old with respect to the new set. This leads to the following possible situations:

- Old and new agree on a pair. I.e. old eddy O_a has a closest neighbour in the new set N_a and N_a agrees that O_a is the closest eddy from the old set. Hence the eddy is tracked. N_a is O_a at a later time.
- N_a claims O_a to be the closest, but N_b makes the same claim. I.e. two eddies from the new set claim one eddy from the old set to be the closest. In this situation the closer one is decided to be the old one at a later time-step and the other one must be a newly formed eddy.
- At this point all new eddies are either allocated to their respective old eddies or assumed to be *newly born*. The only eddies that have not been taken care of are those from the old set, that *lost* ambiguous claims to another old eddy, that was closer to the same claimed new eddy. I.e. there is no respective new eddy available which must mean that the eddy just *died*. In this case the entire track with all the information for each time step is saved as long as the track-length meets the threshold criterium. If it doesn't, the track is deleted.

2.7 Step S05: Cross Reference Old to New Indices

```
function function S05_init_output_maps
```

The main purpose of this step is to allocate all grid nodes of the input data to the correct node of the output map. Since the output map is usually much coarser than the input data there is no need for interpolation.

2.8 Step S06: Make Maps of Mean Parameters

```
function function S06_analyze_tracks
```

2.9 Example

To show a hands-on example an exemplary run for part of the North Atlantic is demonstrated in the following.

2.9.1 Map Parameters

The geo-coordinates for the map window are to be set in `map_vars.m`. In this case a small region in the eddy-rich North Atlantic from -90° west till -40° west and from 20° north till 60° north is chosen. This script has an effect only on the very first step (`s_00...`).

```
function MAP=map_vars
    %% user input
    MAP.geo.west=-90;
    MAP.geo.east=-40;
    MAP.geo.south=20;
    MAP.geo.north=60;
    MAP.time.delta_t = 1; % [days]
    MAP.SSH.unitFactor = 100; % eg 100 if SSH data in cm, 1/10 if in deka m etc..
    MAP.pattern.in='SSH_GLB_t.t0.1.421_CORE.yyyymmdd.nc';
end
```

show map

2.9.2 Other Parameters

All other parameters are to be set in `input_vars.m`.

- The maximum number of *local workers* (threads) is at default settings usually limited to 12 by Matlab. Hence

```
U.threads.num=12;
```

- The data available at this point in time spans from 1994/04/02 till 2006/12/31. Hence

```
U.time.from.str='19940402';
U.time.till.str='20061231';
```

- Data is available per day. Therefor `U.time.delta_t=1;` is set to 1. This could also be changed to another value, if the user wished to skip time-steps.
- The path `U.path.root='../../dataXMPL/'`; can be set arbitrarily. If it does not yet exist, it will be created. It is suggested to not reuse a path, as this could lead to inconsistencies in the data.

U.path.TempSalt.name='TempSalt/';

- `U.path.raw.name='/scratch/uni/ifmto/u241194/DAILY/EULERIAN/SSH/'`;
This is where the SSH data is stored.

```
• U.contour.step=0.01; % [SI]
U.thresh.radius=5e3; % [SI]
U.thresh.amp=0.02; % [SI]
U.thresh.shape.iq=0.5; % isoperimetric quotient
U.thresh.shape.chelt=0.5; % (diameter of circle with equal area)/(maximum
distance between nodes) (if ~switch.IQ)
U.thresh.corners=6; % min number of data points for the perimeter of an eddy
U.thresh.dist=1*24*60^2; % max distance travelled per day
U.thresh.life=20; % min num of living days for saving
```

In this segment the following values are set (all in SI-units, except for time dimension).:

- The contour intervall with which to look for SSH-contours from maximum to minimum SSH-value.

- The minimum radius threshold for an eddy.
- The minimum amplitude threshold.
- Either the minimum `IQ` value or the minimum ratio of the diameter of a circle with equal area over the maximum distance between nodes, depending on which method is chosen (see).
- The minimum number of grid nodes making up the contour.
- The maximum distance-travelled-per-timestep threshold.
- The minium track-length (in time) threshold for a track to be saved.

```
U.dim.X=40*3+1;
U.dim.Y=40*3+1;
U.dim.west=-90;
U.dim.east=-50;
U.dim.south=20;
U.dim.north=60;
U.dim.NumOfDecimals=1;
```

These paramters describe the output maps, that will be created in the very end (e.g. maps of mean values). Ideally they are set to the same limits as those set in 2.9.1. `U.dim.X/U.dim.Y` dictate the size of the output maps. They can be set arbitrarily, but the format e.g. $(east-west)*n+1; n \in \mathbb{N}$ is suggested to avoid long decimals in the coordinate matrices.

- `U.switchs.RossbyStuff=false;`
`U.switchs.IQ=true;`

Choose whether step `S01b_BruntVaisRossby` is to be run (needs adequate salt and temperature files) and the type of shape-testing (`U.switchs.IQ=true`) for `IQ`-method.

explain

- The rest are less important technical things that are only relevant if the code itself is modulated (e.g. if modules are added).

2.9.3 Running the Code

The seperate steps can be run all at once via `Sall.m` or one by one, as long as they are started consecutively in the order indicated by their name (`S00..`, then `S01..` etc.). `S01b` is not necessary though. Each step saves its own files which are then read by the next step. All output data is saved in the user given root-path from 2.9.2. This concept uses quite a lot of disk space and is also quite substantially slowed by all the reading and writing procedures. The benefits, on the other hand, are that debugging becomes much easier. If the code fails at some step, at least all the calculations up to that step are dealt with and do not need to be re-run. The concept also makes it easy to extend the code by further add-ons.

see github for progress

plots to follow...

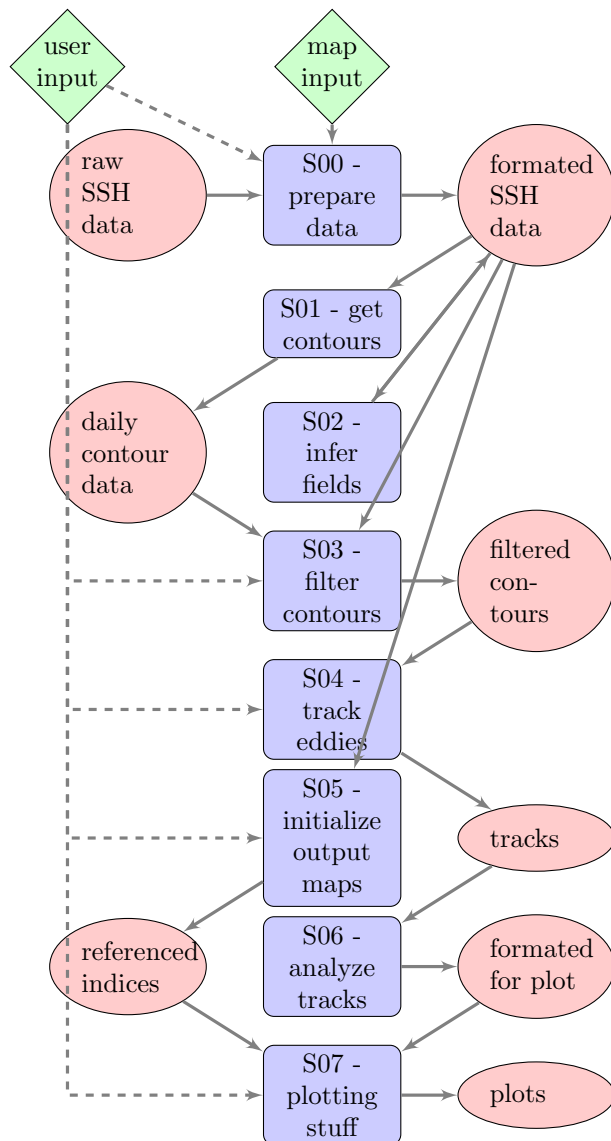


Figure 2.3: Basic code structure. Input is green, code is blue and data is red.

Chapter 3

Results

results...

Chapter 4

Discussion

discussion...

Appendix A

Turbulence Aspects

Consider the equations of motion on a rotating spherical planet with all body forces combined in \mathbf{g} , which shall always be perpendicular to the surface of a Newtonian fluid at rest. Applying the curl to equation (A.1a) also yields a vorticity equation¹. Scalar multiplication with \mathbf{u} reveals a prognostic, macroscopic kinetic-energy-per-unit-mass budget². Analogously, scalar multiplication of equation (A.2c) with ω_a yields an equation for the macroscopic enstrophy density per unit mass³. Finally, adding a term for potential energy to equation (A.1d) yields an equation for mechanical energy⁴.

$$\frac{D\mathbf{u}}{Dt} + \boldsymbol{\Omega} \times \mathbf{u} = -\frac{1}{\rho} \nabla p + \nu \nabla^2 \mathbf{u} + \mathbf{g} \quad (\text{A.1a})$$

$$\frac{Dm}{Dt} = 0 \quad (\text{A.1b})$$

$$\frac{D\omega_a}{Dt} = (\omega_a \cdot \nabla) \mathbf{u} + \mathbf{B} + \nu \nabla^2 \omega \quad (\text{A.1c})$$

$$\frac{DE_k}{Dt} = -\mathbf{u}_h \cdot \frac{1}{\rho} \nabla_h p + \nu \left(\frac{1}{2} \nabla^2 \mathbf{u}^2 - \|\nabla \mathbf{u}\|^2 \right) \quad (\text{A.1d})$$

$$\frac{DE_m}{Dt} = \nu \left(\frac{1}{2} \nabla^2 \mathbf{u}^2 - \|\nabla \mathbf{u}\|^2 \right) \quad (\text{A.1e})$$

$$\frac{D\varepsilon}{Dt} = \omega \cdot (\omega_a \cdot \nabla) \mathbf{u} + \omega \cdot \nu \nabla^2 \omega \quad (\text{A.1f})$$

Turbulence A.1: Non-rotating Tank

Consider first a 3 dimensional non-rotating volume of fluid of constant density with horizontal and vertical dimensions of equal scale. Equations (A.1) then reduce to (ignoring E_k):

$$\frac{D\mathbf{u}}{Dt} = -\frac{1}{\rho} \nabla p + \nu \nabla^2 \mathbf{u} + \mathbf{g} \quad (\text{A.2a})$$

$$\nabla \cdot \mathbf{u} = 0 \quad (\text{A.2b})$$

$$\frac{D\omega}{Dt} = (\omega \cdot \nabla) \mathbf{u} + \nu \nabla^2 \omega \quad (\text{A.2c})$$

$$\frac{DE_m}{Dt} = \nu \left(\frac{1}{2} \nabla^2 \mathbf{u}^2 - \|\nabla \mathbf{u}\|^2 \right) \quad (\text{A.2e})$$

$$\frac{D\varepsilon}{Dt} = \omega \cdot (\omega \cdot \nabla) \mathbf{u} + \omega \cdot \nu \nabla^2 \omega \quad (\text{A.2f})$$

If we further assume the viscosity ν of the fluid to be infinitely small equation (A.2e) and equation (A.2f) reduce to

$$\frac{DE_m}{Dt} = 0 \quad (\text{A.3e})$$

$$\frac{D\varepsilon}{Dt} = \omega \cdot (\omega \cdot \nabla) \mathbf{u} \quad (\text{A.3f})$$

¹see Derivation 1

²see Derivation 2

³see Derivation 4

⁴see Derivation 3

In the absence of friction the mechanical Energy of the parcel of fluid is conserved.

In contrast, neither enstrophy nor vorticity itself are conserved. Velocity gradients will tilt and stretch the parcel resulting in changes in relative vorticity so as to conserve the parcel's total angular momentum. There is no preference for dimension. The motion is simply turbulent akin to air blowing through a room.

Turbulence A.2: Rotating Tank

Next consider the tank from A.1 to be rotating at some high constant frequency $\Omega/2 \cdot \mathbf{k} = \Omega/2$, so that all terms void of $\boldsymbol{\Omega}$ are small versus those containing $\boldsymbol{\Omega}$ while all derivatives of $\boldsymbol{\Omega}$ vanish for its constancy. Again, imagine some magical mix of body forces, so that $\mathbf{g} \cdot \mathbf{k} = -g$.

$$\frac{D\mathbf{u}_h}{Dt} = -\boldsymbol{\Omega} \times \mathbf{u}_h + g\boldsymbol{\nabla}\eta \quad (\text{A.4a})$$

$$\frac{D\boldsymbol{\omega}}{Dt} = \Omega \frac{\partial \mathbf{u}}{\partial z} \quad (\text{A.4c})$$

$$\frac{DE_m}{Dt} = \nu \left(\frac{1}{2} \boldsymbol{\nabla}^2 \mathbf{u}^2 - \|\boldsymbol{\nabla} \mathbf{u}\|^2 \right) \quad (\text{A.4e})$$

$$\frac{D\varepsilon}{Dt} = \boldsymbol{\omega} \cdot \Omega \frac{\partial \mathbf{u}}{\partial z} \quad (\text{A.4f})$$

Equation (A.4a) reveals that in this case all motion must be perpendicular to $\boldsymbol{\Omega}$ and to pressure gradients. Hence $w \approx 0$ and \mathbf{u}_h in hydrostatic- and geostrophic balance. Equation (A.4c) shows how a stretched or squeezed water column by e.g. a change in water depth results in a dramatic change in relative vorticity. Equation (A.4e) and equation (A.4f) show that again energy is conserved for the $\text{Re} \gg 1$ case (since our perspective is from the rotating frame of reference, the angular momentum from the rotating tank is a priori irrelevant to E_m), and that local enstrophy of a Lagrangian parcel is dramatically changed as soon as the vertical dimension is forced upon the motion.

Turbulence A.3: Small Aspect Ratio

Consider again the tank, only this time completely flattened, so that its horizontal extent is, say, 3 orders of magnitude larger than its vertical scale. All vertical motion then becomes insignificant and the equations at first approximation reduce to:

$$\frac{\partial \mathbf{u}}{\partial t} + \mathbf{u} \cdot \boldsymbol{\nabla} \mathbf{u} = g\boldsymbol{\nabla}\eta + \nu \boldsymbol{\nabla}^2 \mathbf{u} \quad (\text{A.5a})$$

$$\frac{\partial \boldsymbol{\omega}}{\partial t} + \mathbf{u} \cdot \boldsymbol{\nabla} \boldsymbol{\omega} = \nu \boldsymbol{\nabla}^2 \boldsymbol{\omega} \quad (\text{A.5c})$$

$$\frac{DE_m}{Dt} = \nu \left(\frac{1}{2} \boldsymbol{\nabla}^2 \mathbf{u}^2 - \omega^2 \right) \quad (\text{A.5e})$$

$$\frac{D\varepsilon}{Dt} = \nu \left(\frac{1}{2} \boldsymbol{\nabla}^2 \omega^2 - \|\boldsymbol{\nabla} \omega\|^2 \right) \quad (\text{A.5f})$$

The main point here is that now, for infinitely small viscosity, besides mechanical energy, now also enstrophy is materially conserved. Lacking a third dimension to stretch, squeeze or tilt into, a column of fluid has no mechanism by which to adapt to a change in depth or to a change in ambient vorticity. To investigate this situation further a scale analysis of the equations of E_m and ε is helpful:

$$\frac{U^2}{T} + \frac{U^3}{L} = \frac{\nu U^2}{L^2} \quad (\text{A.6e})$$

$$\frac{U^2}{TL^2} + \frac{U^3}{L^3} = \frac{\nu U^2}{L^4} \quad (\text{A.6f})$$

Apparently $\frac{DE_m}{Dt} \sim L^2 \frac{D\varepsilon}{Dt}$. Thus, the smaller L the more effective vorticity is advected and burned. Hence enstrophy dominates the turbulence cascade towards smaller scales. Before E_m gets any chance to cascade itself to ever smaller scales, ε is already effectively burning vorticity at large k and thereby reducing kinetic energy faster than the turbulence cascade can fill the gap. E_m being proportional to U^2 cannot compete with ε at small scales since ε not only scales with U^2 but also with the squared reciprocal of the scale *itself*.

As an analogy consider an ice hockey arena being opened instantaneously to 500 people on skates. At first the picture will be highly turbulent with lots of friction among skaters. Sooner or later though, people of like-minded preference for direction and speed are likely to form groups so as to avoid bumping into one another. At some point usually all the people form into one or few large eddies, with those wanting to go faster than others skating at larger radius than the more timid towards

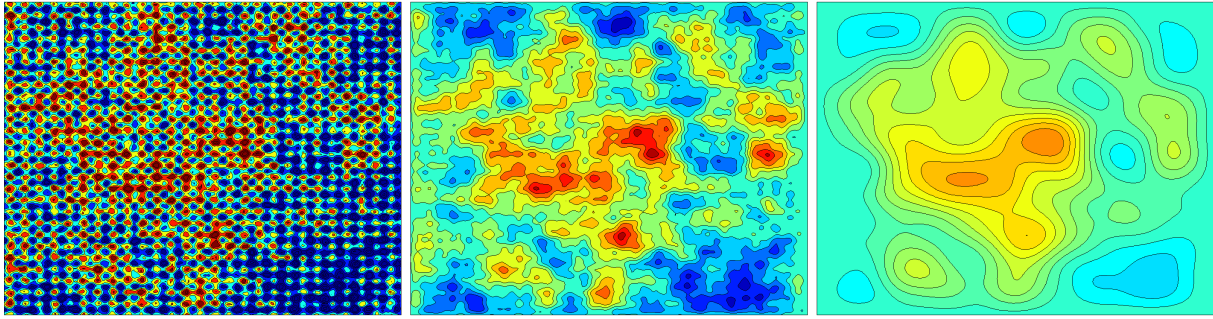


Figure A.1: 1) 2D turbulence with several sinusoidal and random signals as initial condition, 2) at a later time 3) at a much later time. Code from ?.

the center, whilst those on inadequate orbits usually get automatically advected accordingly.

Turbulence A.4: β -effect

Consider at last the inviscid rotating flat-disk-type tank this time in the shape of a shell of a sphere with again $\mathbf{g} \parallel \mathbf{z}$ everywhere perpendicular to the surface at rest. Further assume a strong \mathbf{g} so that the $\boldsymbol{\Omega} \cdot \mathbf{y}$ component in the Coriolis term is dwarfed by hydrostaticity. Then with $\mathbf{f} = f\mathbf{z} = (\boldsymbol{\Omega} \cdot \mathbf{z})\mathbf{z}$ now from an Eulerian perspective:

$$\frac{\partial \mathbf{u}}{\partial t} = -\mathbf{u} \cdot \nabla \mathbf{u} - \mathbf{f} \times \mathbf{u} + g \nabla \eta \quad (\text{A.7a})$$

$$\frac{\partial \boldsymbol{\omega}}{\partial t} = -\mathbf{u}_h \cdot \nabla_h \boldsymbol{\omega} - v \frac{\partial f}{\partial y} \quad (\text{A.7c})$$

A new term with opposite sign from the ω -advection-term in y -direction arises in the vorticity budget, which is evidently most significant where f changes strongest meridionally, i.e. In proximity to the sphere's *equator*. Hence, if scales permit, relative vorticity can now also be altered by a change in latitude via conservation of angular momentum.

Appendix B

Eddy Categories

Starting from the considerations for equations (A.7) and introducing a variable density, the momentum equations and the z -component of the vorticity equation read:

$$\left(\frac{\partial \mathbf{u}}{\partial t}\right)^i + (\mathbf{u} \cdot \nabla \mathbf{u})^{ii} + (\mathbf{f}_0 \times \mathbf{u})^{iii} + (\beta y \times \mathbf{u})^{iv} = (-g \nabla h)^v \quad (\text{B.1a})$$

$$\nabla \cdot \mathbf{u} = 0 \quad (\text{B.1b})$$

$$\left(\frac{D\omega}{Dt}\right)^A + \left(\frac{Df}{Dt}\right)^B = \left(f \frac{\partial w}{\partial z}\right)^C + \left(\omega \frac{\partial w}{\partial z}\right)^D \quad (\text{B.1c})$$

Several balances between terms to maintain vortices are thinkable here:

Vortex B.1: Frontal Lenses

large: R_β , Bu , U

small: Ro , W

balance between: ii , iii and v

The case with strong density gradients, large current speeds and a Rossby number approaching unity is typical for the meandering tails of turbulent boundary currents and zonal jets as in the Gulf Stream respective cyclogenesis in the atmospheric jet stream. Technically the intrathermoclinic lenses (?) and strong-density-gradient deep eddies e.g. *meddies* fall into this group as well. With strong stratification, small vertical displacements cause strong pressure gradients. The dynamics can be limited to some thin layer, bottom topography is of little relevance and the surface signal might be small, or misleading.

Vortex B.2: Small Mid-Latitude Geostrophic Eddies

large: R_β

$O1$: Bu

small: Ro

balance between: iii and v

The true geostrophic eddy with $L \sim L_R \sim NH/f$.

Vortex B.3: Large Geostrophic Gyres

small: Ro , R_β , Bu

balance between: iii , iv , v and friction

The large-scale wind-driven ocean gyres. These can only be interpreted as an *eddy* from the Reynolds-averaged large-scale perspective. The motion is strongly f/H -contour guided and the β -effect is immediately apparent in their strong western boundary intensification.

Vortex B.4: the *Rossby-wave-eddy*

large: L

$O1$: Bu

small: Ro , R_β

balance between: iii, iv and v

In low latitudes quasi-geostrophy and hence a small Rossby number demand large L and/or small

U . The pressure gradients and hence surface elevation is small. Due to the large meridional extent, slow time-scale and strong $f(y)$ -gradient, particles moving north or south experience strong changes in planetary vorticity. So much so, that in this regime geostrophic eddies and Rossby waves are no longer clearly separable phenomena.

Vortex B.5: bonus: *tornado*

large: $U, g', L_R, \text{Ro}, \text{Bu}, R_\beta$

small: L

balance between: ν and v

significant vorticity term: A and friction (not considered here)

This case isn't really applicable to the ocean except for maybe the tropics where f vanishes (but ν would become relevant) or on small scales in areas of strong tidal currents in combination with bathymetry i.e. *tidal bores* etc. In this case a pressure force would have to be balanced by a centrifugal force alone (e.g. *bathytub*).

Appendix C

Further Papers

??

? set the foundation for today's standard parametrization of eddy-mixing in non-eddy-resolving general circulation models ¹. Essentially, they argue that a plain Fickian diffusion-type parametrization of the form $K\nabla\mathbf{u}$ is inadequate since \mathbf{u} only represents the large-scale flow. Instead the relevant velocity for eddy-diffusion is the sum of mean flow and eddy-induced flow ² $\mathbf{U} = \bar{\mathbf{u}} + \bar{h}'\mathbf{u}'/\bar{h}_\rho = \bar{\mathbf{u}} + \mathbf{u}^*$ with $h(x, y, \rho, t)$ as the physical height of an isopycnal and h_ρ the equivalent in isopycnal coordinates and $\frac{D^*}{Dt} = \frac{\partial}{\partial t} + \mathbf{U}\nabla$ as the material derivative with respect to \mathbf{U} instead of \mathbf{u} . In their assumption, analogous to adiabatic eddy mixing of passive tracers, the turbulence, itself *sitting adiabatically* on the large scale density surfaces, redistributes thickness anomalies *quasi-adiabatically* along *quasi-neutral* surfaces. I.e. the integrated turbulent eddy activity effectively smears large-scale density gradients at the rate of the bolus velocity, akin to a Fickian diffusion of a passive tracer. With the momentum equations reduced to the large-scale, inviscid, incompressible and stationary, the entire dynamics can be represented via the prognostic advection-diffusion equation for h_ρ :

$$\rho_0 f \mathbf{k} \times \mathbf{u} = -\nabla p \quad (\text{C.1a})$$

$$\frac{D^* \rho}{Dt} = 0 \quad (\text{C.1b})$$

$$\nabla^* \cdot \mathbf{U}^* = 0 \quad (\text{C.1c})$$

$$h \frac{D^* \tau}{Dt} = (\nabla \cdot (h \mu \nabla \tau))^* \quad (\text{C.1g})$$

$$\mathbf{u}_h^* = \frac{\partial}{\partial z} \left(K \nabla \rho / \frac{\partial \rho}{\partial z} \right) \quad (\text{C.1h})$$

$$w^* = -\nabla \cdot \left(K \nabla \rho / \frac{\partial \rho}{\partial z} \right) \quad (\text{C.1i})$$

solve for h instead of ρ in mass budget

Equation (C.1g) is the tracer equation with μ , analogous to K , as an unknown diffusion coefficient and all $*$ indicating a transformation to the isopycnal frame of reference. If K is taken as constant the potential vorticity equation reduces to

$$\frac{D^* f \partial \rho / \partial z}{Dt} = K \nabla_\rho \cdot \left(f h_\rho \nabla_\rho \frac{\partial \rho}{\partial z} \right) / h_\rho \quad (\text{C.2})$$

Hence under the assumption of exact Fickian thickness diffusion, potential vorticity is diffused as if it were a passive tracer, too. Intuitively this sounds absurd and counter-Newtonian since vorticity is intrinsically linked to velocity itself. It must be kept in mind though, that this diffusion stems solely from the bolus velocity, the vorticity of which is only a fraction of the vorticity of the mean state. On scales much larger than the baroclinic Rossby radius, the baroclinic eddy dynamics are so far decoupled from the mean barotropic flow in terms of their scales that, in this assumption, they simply drift along on it, unaffected. In other words, from a frame of reference that is advected with the mean flow, the eddy-induced dynamics are assumed to have a large ratio of local to pseudo forces. Nevertheless, aforementioned simplification does indeed technically violate conservation of angular momentum (?).

reminiscent of QPVE, try again later..

¹general circulation models will hereafter be abbreviated GM.

²which will hereafter be called *bolus velocity* in line with ? who coined the term

?

? investigated vorticity-fluxes in k -space using a simple two-layer quasi-geostrophic model with domain dimensions much larger L_R , in order to avoid a scale limiting basin-size. Their finding is that, contrary to theory, that predicts a flux of baroclinic potential vorticity from large scales where it is excited down-gradient to L_R where it feeds into the barotropic mode, and thence back up the red cascade, both energy production and strongest vorticity fluxes are strongest towards the largest scales of the flow and not at L_R . They therefore argue that instead of concentrating on eddies at scale L_R , focus should really be on the largest scale the inverse cascade extends to, be that an arrest scale via β or via some threshold beyond which eddies abandon turbulent regions, by for instance the effects outlined by ?.

?

? argues that SSH-variability is mostly representative of the first baroclinic mode since, under the assumption that kinetic energy be roughly equally partitioned between barotropic and baroclinic mode, the first baroclinic mode, being representative of strong density gradients, is primarily concentrated towards the surface (?).

maybe show derivation from vallis...

Geostrophic turbulence theory predicts an inverse cascade for the barotropic mode, yet a direct cascade for the first baroclinic mode from large scales towards L_R (?). Hence satellite SSH-products should show a direct cascade in regions of excitations of geostrophic turbulence on scales larger than L_R . Curiously, evidence of the opposite was found by e.g. ??, somewhat affirming the findings of ?. ? therefore argue that *Because the growth in scale is extending well beyond $2\pi L_R$, especially for the zonal velocity, even in these subtropical regions³, we claim there is an unresolved, and indeed unappreciated, contradiction between stratified geostrophic turbulence theory and observations. Furthermore, ? also claim to observe the eddies evolving into zonally elongated, wavelike structures, as predicted by ?.* But again, theory holds this to be a barotropic mode phenomenon that does not apply to the baroclinic modes. With regard to the last point ? suggest that the apparent arrest may arise from *barotropization, which transfers the energy down the water column, reducing the surface signal.*

ref to here later - argument for further tracking depth

?

? inferred eddy scales in the north-Atlantic from kinetic energy densities in k -space and spatial decorrelations. They detect two different regimes that are meridionally separated by $L_R = L_\beta$. South of this dividing line, they find small-Rhines-number-type anisotropic scales, whereas the scales due north show proportionality to the Rossby-radius. They therefore suggest to use $L = \min(L_\beta, L_R)$ instead of L_R as the characteristic length scale in parametrizations. This meridional wave/eddy-dualism was already proposed by ?, who noted that the L_β becomes important when the phase speed at which Rossby waves displace particles is of same order as the turbulent velocity scale, i.e. when $U \sim \beta L_R$ ² and hence $U/\beta = L_\beta^2 \sim L_R^2$. Or quoting ?: *The central idea of the Rhines effect is that, as eddies grow in the inverse cascade, their timescale slows, and when this timescale matches the frequency of Rossby waves with the same spatial scale, turbulent energy may be converted into waves, and the cascade will slow tremendously*

???

Theoretically the approximated, parametrized equations can be solved for the thickness diffusivity K , which can then be determined from e.g. fine-grid model results. One problem with this is that it is only the along-gradient component of the flux that is of interest. However the cross-gradient term proportional to $\mathbf{k}_h \times \nabla_h \rho_h$ integrates to non-zero in the parametrization when anisotropic fluxes are considered. This term is mute to the tracer budget as it has, by definition, zero divergence and is thus not necessary in the parametrization and in general assumed to be zero. It does however affect the opposite operation of estimating K from data. Ignoring this term results in negative thickness diffusivities in regions where e.g. eddies merge back into jets or more more general anywhere where the transfer of mean potential energy to eddy kinetic energy is reversed. If one were to interpret the thickness flux in direct analogy to the frictional term in the momentum equations, negative K would be analogous to a negative viscosity i.e. a reversal of a diffusive process and one would run into complications regarding fundamental thermodynamic principles. After all a negative K is physically implausible in light of the general assumption that $K \sim UL$. ??? decomposed K into its along and cross gradient component and calculated their values from model

³with reference to ?

data with emphasis on the southern ocean. It turns out that the rotational component is indeed significant at the outer flanks of the ACC i.e. in regions of strong interaction between mean flow and eddies. ??? also indicate that the adiabatic assumption is unrealistic in proximity to the mixed layer where eddies also induce significant diapycnal fluxes in depths that are substantially influenced by e.g. the surface heat flux.

?

As noted in 1.2.3, interpreting SSH-signals in terms of long Rossby waves results in a discrepancy in observed and predicted phase speeds. ? therefore flipped the chain of arguments by fitting quasi-geostrophic theory to observed phase speeds and correcting for mean-flow Doppler shifts, thereby setting constraints on the possible wave lengths and vertical structure. Furthermore they use climatological mean velocity and density data to construct the vertical eigenfunctions for the long-wave-dispersion-relation and then extract the vertical profiles of the observed velocities, assuming that they project entirely onto the first baroclinic mode ⁴. This way they can scale observed $u_{rms}(z)$ from drifter data by their respective factor from the vertical mode. The resultant corrected velocities and scales are in approximate agreement with ? and ?. They conclude that the vast majority of the mid- to high-latitude world ocean is baroclinically unstable and characterized by an inverse energy cascade fed by geostrophic turbulence at deformation scale. In Regions characterized by small Rhines number, on the other hand, the turbulence eventually grows to Rhines scale where it blends in with Rossby waves.

???

A linear stability analysis is particularly suitable for the analysis of eddy diffusivities since it describes deviations from a mean state, by definition. Linearizing the quasi-geostrophic stream function about a laterally *quasi*-constant ⁵ mean state i.e. applying a perturbation ansatz to the equations leads to a vertical Sturm-Liouville-type eigenvalue problem. Motivated by the work of ?, ??? rigorously solved the problem for its vertical modes and derived values for buoyancy and potential vorticity diffusivities for either the world ocean or specific regions of interest. They construct the amplitude of the resultant perturbation stream function as a linear function of the imaginary part of the phase speed and the wavelength of the fastest growing mode, scaled by a constant parameter, suggested to link the length scales of unstable wave and resultant eddy ⁶. One of their most interesting findings is that a zonal mean flow has two main effects on eddy diffusivities:

- An eastward flow and a positive shear ($\frac{\partial \bar{u}}{\partial y}$) decrease skew diffusivity⁷ \underline{K} and shift it along with the steering level down vertically.
- A westward flow and negative shear effect the opposite.
- A large β also intensifies \underline{K} towards the surface.

All of this makes intuitively sense. \underline{K} is only non-zero when total thickness-diffusivity is anisotropic i.e. when net turbulence does not cancel out laterally. This happens when eddies prefer one direction over another. As was shown by ? meso-scale eddies need to always migrate west in order to balance forces symmetrically. This is why they have shorter life times and a tendency to hide at depth in the ACC and why values for \underline{K} are large in the strongly vertically stratified ($\frac{\partial \bar{u}}{\partial z} < 0$) westward equatorial current.

⁴see ?

⁵*quasi* in the sense that e.g. ? allowed for horizontal variations of the mean state iteratively via a WKBJ approximation.

⁶the difference is assumed to be a result of the inverse cascade.

⁷i.e. the rotational part of thickness diffusivity as mentioned in C

Appendix D

Derivations

Derivation 1: Vorticity

With the identity

$$\begin{aligned}\mathbf{u} \cdot \nabla \mathbf{u} &= (\nabla \times \mathbf{u}) \times \mathbf{u} + \nabla |\mathbf{u}|^2 / 2 \\ &= \boldsymbol{\omega} \times \mathbf{u} + \nabla \mathbf{u}^2 / 2\end{aligned}\quad (\text{D.1})$$

equation (A.1a) becomes

$$\begin{aligned}\frac{\partial \mathbf{u}}{\partial t} + \nabla |\mathbf{u}|^2 / 2 + (2\boldsymbol{\Omega} + \boldsymbol{\omega}) \times \mathbf{u} &= -\frac{1}{\rho} \nabla p + \nu \nabla^2 \mathbf{u} + \mathbf{g} \\ \frac{\partial \mathbf{u}}{\partial t} + \nabla |\mathbf{u}|^2 / 2 + \boldsymbol{\omega}_a \times \mathbf{u} &= -\frac{1}{\rho} \nabla p + \nu \nabla^2 \mathbf{u} + \mathbf{g}\end{aligned}\quad (\text{D.2})$$

Applying the curl operation to equation (A.1a) and assuming equation (A.1b) for an incompressible fluid yields and equation for the vorticity

$$\begin{aligned}\frac{\partial \boldsymbol{\omega}}{\partial t} + \nabla \times \nabla |\mathbf{u}|^2 / 2 + \nabla \times (\boldsymbol{\omega}_a \times \mathbf{u}) &= -\frac{1}{\rho} \nabla \times \nabla p - \nabla \rho^{-1} \times \nabla p + \nu \nabla \times \nabla^2 \mathbf{u} + \nabla \times \mathbf{g}\end{aligned}\quad (\text{D.3})$$

Annihilating all $\nabla \times \text{grad}$ and $\nabla \cdot \nabla \times$ and making use of the identity

$$\nabla \times (\mathbf{A} \times \mathbf{B}) = \mathbf{A} (\nabla \cdot \mathbf{B}) - \mathbf{B} (\nabla \cdot \mathbf{A}) + (\mathbf{B} \cdot \nabla) \mathbf{A} - (\mathbf{A} \cdot \nabla) \mathbf{B} \quad (\text{D.4})$$

equation (D.3) becomes

$$\begin{aligned}\frac{\partial \boldsymbol{\omega}}{\partial t} + \nabla \times (\boldsymbol{\omega}_a \times \mathbf{u}) &= -\frac{\nabla \rho \times \nabla p}{\rho^2} + \nu \nabla \times \nabla^2 \mathbf{u} \\ \frac{\partial \boldsymbol{\omega}}{\partial t} + (\mathbf{u} \cdot \nabla) \boldsymbol{\omega}_a - \mathbf{u} (\nabla \cdot \boldsymbol{\omega}_a) - (\boldsymbol{\omega}_a \cdot \nabla) \mathbf{u} &= \mathbf{B} - \nu \nabla \times (\nabla \times (\nabla \times \mathbf{u})) \\ \frac{D \boldsymbol{\omega}_a}{Dt} &= (\boldsymbol{\omega}_a \cdot \nabla) \mathbf{u} + \mathbf{B} - \nu \nabla \times (\nabla \times \boldsymbol{\omega}) \\ &= (\boldsymbol{\omega}_a \cdot \nabla) \mathbf{u} + \mathbf{B} + \nu \nabla^2 \boldsymbol{\omega}\end{aligned}\quad (\text{D.5})$$

Scaling considerations based on the small aspect ratio e.g. noting that $\mathbf{B} \sim \nabla p \times \nabla \rho$ is at first approximation limited to the x, y plane and that $U/H \gg W/L$ and assuming $\omega_z \gg \omega_h$, leads to:

$$\frac{\partial \boldsymbol{\omega}}{\partial t} + \mathbf{u} \cdot \nabla \boldsymbol{\omega} + \beta v \hat{\mathbf{z}} = (\omega_z + f) \frac{\partial \mathbf{u}}{\partial z} + \mathbf{B} \quad (\text{D.6})$$

horizontal:

$$\begin{aligned}\frac{1}{T} \frac{U}{H} + \left(\frac{U}{L} + \frac{W}{H} \right) \frac{U}{H} &\sim \frac{U}{H} \frac{U}{L} + f \frac{U}{H} + \mathbf{B} \\ \Rightarrow \frac{U}{HT} + \frac{U^2}{LH} + \frac{UW}{H^2} &\sim \frac{U^2}{LH} + f \frac{U}{H} + \mathbf{B}\end{aligned}\quad (\text{D.7})$$

vertical:

$$\begin{aligned}\frac{U}{LT} + \frac{U^2}{L^2} + \frac{WU}{HL} + \beta V &\sim \frac{UW}{LH} + f \frac{W}{H} \\ \Rightarrow \frac{U}{LT} + \frac{U^2}{L^2} + \beta V &\sim \frac{WU}{HL} + f \frac{W}{H}\end{aligned}\quad (\text{D.8})$$

Hence at first order:

$$\frac{D\omega_h}{Dt} = (f + \omega_z) \frac{\partial \mathbf{u}_h}{\partial z} + \mathbf{B} \quad (\text{D.9})$$

$$\frac{D\omega_z}{Dt} + \beta v = (f + \omega_z) \frac{\partial w}{\partial z} \quad (\text{D.10})$$

ω_h is due to small ageostrophic parallelization of ∇p and $\nabla \rho$ via B the tilting terms vanish, since then ω_h normal to the plane spanned by $\nabla \mathbf{u}_h$ and ∇w

Derivation 2: Kinetic Energy

Multiply equation (A.1a) by \mathbf{u} :

$$\begin{aligned} \mathbf{u} \cdot \left(\frac{\partial \mathbf{u}}{\partial t} + \mathbf{u} \cdot \nabla \mathbf{u} + 2\Omega \times \mathbf{u} \right) &= -\mathbf{u} \cdot \frac{1}{\rho} \nabla p + \mathbf{u} \cdot \nu \nabla^2 \mathbf{u} + \mathbf{u} \cdot \mathbf{g} \\ \frac{1}{2} \frac{\partial \mathbf{u}^2}{\partial t} + \frac{1}{2} \mathbf{u} \cdot \nabla \mathbf{u}^2 + \mathbf{u} \cdot 2\Omega \times \mathbf{u} &= -\mathbf{u} \cdot \frac{1}{\rho} \nabla p + \mathbf{u} \cdot \nu \nabla^2 \mathbf{u} - wg \\ \frac{1}{2} \frac{\partial \mathbf{u}^2}{\partial t} + \frac{1}{2} \mathbf{u} \cdot \nabla \mathbf{u}^2 &= -\mathbf{u}_h \cdot \frac{1}{\rho} \nabla_h p + wg + \mathbf{u} \cdot \nu \nabla^2 \mathbf{u} - wg \\ \frac{1}{2} \frac{\partial \mathbf{u}^2}{\partial t} + \frac{1}{2} \mathbf{u} \cdot \nabla \mathbf{u}^2 &= -\mathbf{u}_h \cdot \frac{1}{\rho} \nabla_h p + \mathbf{u} \cdot \nu \nabla^2 \mathbf{u} \\ \frac{\partial E_k}{\partial t} + \mathbf{u} \cdot \nabla E_k &= -g \mathbf{u}_h \cdot \nabla \eta(x, y) + \nu \left(\frac{1}{2} \nabla^2 \mathbf{u}^2 - \|\nabla \mathbf{u}\|^2 \right) \end{aligned} \quad (\text{D.11})$$

Derivation 3: Mechanical Energy

Add term for potential energy to equation (A.1d) (assuming $\nabla \rho = 0$)

$$\begin{aligned} \frac{DE_m}{Dt} &= -g \mathbf{u} \cdot \nabla \eta(x, y) + \nu \left(\frac{1}{2} \nabla^2 \mathbf{u}^2 - \|\nabla \mathbf{u}\|^2 \right) + \mathbf{u} \cdot \mathbf{g} \\ \frac{DE_m}{Dt} &= -g \mathbf{u} \cdot \nabla \eta(x, y) + \nu \left(\frac{1}{2} \nabla^2 \mathbf{u}^2 - \|\nabla \mathbf{u}\|^2 \right) - wg \\ &= -g \left(\frac{\partial \eta}{\partial t} + \mathbf{u} \cdot \nabla \eta \right) + \nu \left(\frac{1}{2} \nabla^2 \mathbf{u}^2 - \|\nabla \mathbf{u}\|^2 \right) \\ &= -g \frac{D\eta}{Dt} + \nu \left(\frac{1}{2} \nabla^2 \mathbf{u}^2 - \|\nabla \mathbf{u}\|^2 \right) \\ &= \nu \left(\frac{1}{2} \nabla^2 \mathbf{u}^2 - \|\nabla \mathbf{u}\|^2 \right) \end{aligned} \quad (\text{D.12})$$

Derivation 4: Enstrophy

In 2 dimensions the definition of enstrophy can also be rewritten as:

$$\begin{aligned} \mathcal{E} &= \int_A \varepsilon \, dA = \int_A \|\nabla \mathbf{u}\|^2 \, dA \\ &= \int_A \left(\frac{\partial v}{\partial x} \right)^2 + \left(\frac{\partial u}{\partial y} \right)^2 + \left(\frac{\partial v}{\partial y} \right)^2 + \left(\frac{\partial u}{\partial x} \right)^2 \, dA \\ &= \int_A \left(\frac{\partial v}{\partial x} \right)^2 + \left(\frac{\partial u}{\partial y} \right)^2 + \left(\frac{\partial v}{\partial y} \right)^2 + \left(\frac{\partial u}{\partial x} \right)^2 - (\nabla \cdot \mathbf{u})^2 \, dA \\ &= \int_A \left(\frac{\partial v}{\partial x} \right)^2 + \left(\frac{\partial u}{\partial y} \right)^2 - 2 \frac{\partial u}{\partial x} \frac{\partial v}{\partial y} \, dA \\ &= \int_A \omega^2 + 2 \frac{\partial u}{\partial y} \frac{\partial v}{\partial x} - 2 \frac{\partial u}{\partial x} \frac{\partial v}{\partial y} \, dA \\ &= \int_A \omega^2 + 2 \frac{\partial u}{\partial y} \frac{\partial v}{\partial x} + 2 \left(\frac{\partial v}{\partial y} \right)^2 \, dA \end{aligned} \quad (\text{D.13})$$

with $\nabla \cdot \mathbf{u} = 0$ and appropriate boundary conditions, the last two terms cancel in the integral leaving

$$\mathcal{E} = \int_A \omega^2 \, dA \quad (\text{D.14})$$

Derivation 5: Vorticity Scales

Assuming approximate geostrophy and $Bu = \mathcal{O}(10^1)$:

$$\rho f U \sim \nabla p \quad (\text{D.15})$$

in a layered model:

$$\begin{aligned} fU &\sim g' \nabla \eta \\ U &\sim \frac{hN^2}{f} \nabla \eta \\ U &\sim \frac{h^2 N^2}{fL} \end{aligned} \quad (\text{D.16})$$

and hence

$$\begin{aligned} \omega &\sim U/L \sim \frac{h^2 N^2}{fL^2} \\ &= \frac{h^2 N^2}{f L_R^2} \frac{L_R}{L} \\ &= f \frac{L_R}{L} \end{aligned} \quad (\text{D.17})$$

Derivation 6: vortex limitations

$$\mathbf{u} \cdot \nabla \mathbf{u} + f \mathbf{u} = -g \nabla \eta \quad (\text{D.18})$$

$$\begin{aligned} \frac{U^2}{L} + fU + \frac{gh}{L} &= 0 \\ U^2 + fLU + gh &= 0 \end{aligned} \quad (\text{D.19})$$

possible balances: cyclone
 $\text{sgn}(F_c) = \text{sgn}(F_p)$:

$$U_{1,2} = -fL/2 \pm \sqrt{f^2 L^2/4 + gh} \quad (\text{D.20})$$

anti-cyclone

$\text{sgn}(F_c) = -\text{sgn}(F_p)$:

$$U_{1,2} = -fL/2 \pm \sqrt{f^2 L^2/4 - gh} \quad (\text{D.21})$$

$$\begin{aligned} 4gh &\leq f^2 L^2 \\ 2c &\leq fL \\ 2L_R &\leq L \end{aligned} \quad (\text{D.22})$$

Derivation 7: Okubo-Weiss-Parameter

$$\begin{aligned} \mathbb{T} &= \nabla \mathbf{u} \\ &= \frac{\partial u_i}{\partial x_j} \hat{\mathbf{e}}_i \hat{\mathbf{e}}_j \\ &= \frac{1}{2} ((\mathbb{T} + \mathbb{T}^T) + (\mathbb{T} - \mathbb{T}^T)) \\ &= \frac{1}{2} \left(\left(\frac{\partial u_i}{\partial x_j} + \frac{\partial u_j}{\partial x_i} \right) \hat{\mathbf{e}}_i \hat{\mathbf{e}}_j \right) + \frac{1}{2} \left(\left(\frac{\partial u_i}{\partial x_j} - \frac{\partial u_j}{\partial x_i} \right) \hat{\mathbf{e}}_i \hat{\mathbf{e}}_j \right) \end{aligned} \quad (\text{D.23})$$

$$\begin{aligned}
O_w &= \text{Tr } \mathbb{T}^2 = \left(\frac{\partial u_i}{\partial x_k} \frac{\partial u_k}{\partial x_j} \hat{\mathbf{e}}_i \hat{\mathbf{e}}_j \right)_{i,i} \\
&= \frac{\partial u_i}{\partial x_j} \frac{\partial u_j}{\partial x_i} \\
&= \left(\frac{\partial u_i}{\partial x_i} \right)^2 + (1 - \delta_{i,j}) \frac{\partial u_j}{\partial x_i} \frac{\partial u_i}{\partial x_j} \\
&= \left(\frac{\partial u_i}{\partial x_i} \right)^2 + \frac{1}{2} \left(\frac{\partial u_i}{\partial x_j} + \frac{\partial u_j}{\partial x_i} \right)^2 - \frac{1}{2} \left(\frac{\partial u_i}{\partial x_j} - \frac{\partial u_j}{\partial x_i} \right)^2 \\
&= \frac{1}{2} \left(\frac{\partial u_i}{\partial x_i} + \frac{\partial u_j}{\partial x_j} \right)^2 + \frac{1}{2} \left(\frac{\partial u_i}{\partial x_i} - \frac{\partial u_j}{\partial x_j} \right)^2 + \frac{1}{2} \left(\frac{\partial u_i}{\partial x_j} + \frac{\partial u_j}{\partial x_i} \right)^2 - \frac{1}{2} \left(\frac{\partial u_i}{\partial x_j} - \frac{\partial u_j}{\partial x_i} \right)^2 \\
&= \text{divergence}^2 + \text{stretching}^2 + \text{shear}^2 - \text{vorticity}^2
\end{aligned} \tag{D.24}$$

Hence for motion dominated by deformation and shear the system has hyperbolic character, whereas vorticity-dominated motion has parabolic character. Of interest should therefore not only be the value of O_w but also its gradient. An abrupt change in O_w clearly identifies regions of vorticity genesis and decay.

In 2 dimensions:

$$O_w = \left(\frac{\partial u}{\partial x} \right)^2 + 2 \frac{\partial u}{\partial y} \frac{\partial v}{\partial x} \tag{D.25}$$

Derivation 8: Cushman's Drift Speed

$$\begin{aligned}
X_t &= -\frac{\beta g' \int H \eta + \eta^2/2 \, dA}{f_0^2 \int \eta \, dA} \\
&= -\frac{\beta g'}{f_0^2} \left(H + \frac{\int \eta^2/2 \, dA}{V_e} \right) \\
&= -\frac{\beta c^2}{f_0^2} \left(1 + \frac{1}{H} \frac{\int \eta^2/2 \, dA}{V_e} \right) \\
&= -\beta L_R^2 \left(1 + \frac{1}{H} \frac{\int \eta^2 \, dA}{2V_e} \right) \\
&= \frac{\omega_{long}}{k} \left(1 + \frac{1}{H} \frac{\int \eta^2 \, dA}{2V_e} \right)
\end{aligned} \tag{D.26}$$

Derivation 9: Mean Fields of u and b

$$\frac{\partial u_i}{\partial t} \hat{\mathbf{e}}_i + u_j \frac{\partial u_i}{\partial x_j} \hat{\mathbf{e}}_i + \delta_{j3} \epsilon_{jki} f_j u_k \hat{\mathbf{e}}_i = -\frac{\partial p}{\partial x_i} \hat{\mathbf{e}}_i + \nu \frac{\partial^2 u_i}{\partial x_j^2} \hat{\mathbf{e}}_i - \delta_3 g \hat{\mathbf{e}}_i \tag{D.27a}$$

$$\frac{\partial u_i}{\partial x_i} = 0 \tag{D.27b}$$

$$\frac{D\rho}{Dt} = -\frac{\partial J_i^{rad}}{\partial x_i} + \kappa \frac{\partial^2 \rho}{\partial x_i^2} \tag{D.27c}$$

A Reynolds decomposition of equations (D.27) yields

$$\begin{aligned}
\frac{\partial (\bar{u}_i + u'_i)}{\partial t} \hat{\mathbf{e}}_i + (\bar{u}_j + u'_j) \frac{\partial (\bar{u}_i + u'_i)}{\partial x_j} \hat{\mathbf{e}}_i + \delta_{j3} \epsilon_{jki} f_j (\bar{u} + u')_k \hat{\mathbf{e}}_i \\
= -\frac{\partial (\bar{p} + p')}{\partial x_i} \hat{\mathbf{e}}_i + \nu \frac{\partial^2 (\bar{u}_i + u'_i)}{\partial x_j^2} \hat{\mathbf{e}}_i - \delta_3 \bar{g} \hat{\mathbf{e}}_i
\end{aligned} \tag{D.28a}$$

$$\frac{\partial (\bar{u}_i + u'_i)}{\partial x_i} = 0 \tag{D.28b}$$

$$\frac{\partial (\bar{p} + p')}{\partial t} + (\bar{u}_i + u'_i) \frac{\partial (\bar{p} + p')}{\partial x_i} = -\frac{\overline{\partial J_i^{rad}}}{\partial x_i} - \frac{\partial J_i^{rad}'}{\partial x_i} + \kappa \frac{\partial^2 (\bar{p} + p')}{\partial x_i^2} \tag{D.28c}$$

Averaging equations (D.28) yields

$$\begin{aligned} & \frac{\partial(\bar{u}_i + u'_i)}{\partial t} \hat{\mathbf{e}}_i + \\ & \overline{u_j \frac{\partial \bar{u}_i}{\partial x_j}} \hat{\mathbf{e}}_i + \delta_{j3} \epsilon_{jki} f_j (\bar{u} + u')_k \hat{\mathbf{e}}_i + \bar{u_j} u'_i \hat{\mathbf{e}}_i + u'_j \frac{\partial \bar{u}_i}{\partial x_j} \hat{\mathbf{e}}_i + u'_j \frac{\partial u'_i}{\partial x_j} \hat{\mathbf{e}}_i \\ & = - \frac{\partial(\bar{p} + p')}{\partial x_i} \hat{\mathbf{e}}_i + \nu \frac{\partial^2(\bar{u}_i + u'_i)}{\partial x_j^2} \hat{\mathbf{e}}_i - \delta_3 \bar{g} \hat{\mathbf{e}}_i \end{aligned} \quad (\text{D.29a})$$

$$\frac{\partial(\bar{u}_i + u'_i)}{\partial x_i} = 0 \quad (\text{D.29b})$$

$$\frac{\partial(\bar{p} + p')}{\partial t} + \overline{u_j \frac{\partial \bar{p}}{\partial x_j}} + \bar{u_j} \rho' + u'_j \frac{\partial \bar{p}}{\partial x_j} + u'_j \frac{\partial \rho'}{\partial x_j} = - \frac{\partial \bar{J}_i^{rad}}{\partial x_i} - \frac{\partial \bar{J}_i^{rad'}}{\partial x_i} + \kappa \frac{\partial^2(\bar{p} + \rho')}{\partial x_i^2} \quad (\text{D.29c})$$

with $\overline{\overline{()}} = \overline{()}$ and $\overline{()'} = 0$

$$\frac{\partial \bar{u}_i}{\partial t} \hat{\mathbf{e}}_i + \overline{u_j \frac{\partial \bar{u}_i}{\partial x_j}} \hat{\mathbf{e}}_i + \overline{u'_j \frac{\partial u'_i}{\partial x_j}} \hat{\mathbf{e}}_i + \delta_{j3} \epsilon_{jki} f_j \bar{u}_k \hat{\mathbf{e}}_i = - \frac{\partial \bar{p}}{\partial x_i} \hat{\mathbf{e}}_i + \nu \frac{\partial^2 \bar{u}_i}{\partial x_j^2} \hat{\mathbf{e}}_i - \delta_3 \bar{g} \hat{\mathbf{e}}_i \quad (\text{D.30a})$$

$$\frac{\partial \bar{u}_i}{\partial x_i} = 0 \quad (\text{D.30b})$$

$$\frac{\partial \bar{p}}{\partial t} + \overline{u_j \frac{\partial \bar{p}}{\partial x_j}} + u'_j \frac{\partial \bar{p}}{\partial x_j} = - \frac{\partial \bar{J}_i^{rad}}{\partial x_i} + \kappa \frac{\partial^2 \bar{p}}{\partial x_i^2} \quad (\text{D.30c})$$

Focusing solely on deviations from the mean state and assuming horizontal gradients of the mean state to be negligible and hence due to continuity also ${}^a \frac{\partial w}{\partial z} = 0 \rightarrow w = 0$:

$$\delta_h \frac{\partial \bar{u}_i}{\partial t} \hat{\mathbf{e}}_i + w' \frac{\partial \bar{u}'_i}{\partial z} \hat{\mathbf{e}}_i + \delta_h \delta_{j3} \epsilon_{jki} f_j \bar{u}_k \hat{\mathbf{e}}_i = - \frac{\partial \bar{p}}{\partial z} \hat{\mathbf{e}}_z - g \hat{\mathbf{e}}_z \quad (\text{D.31a})$$

$$\frac{\partial \bar{p}}{\partial t} + w' \frac{\partial \bar{p}'}{\partial z} = - \frac{\partial \bar{J}_i^{rad}}{\partial z} + \kappa \frac{\partial^2 \bar{p}}{\partial z^2} \quad (\text{D.31b})$$

returning to vector notation

$$\frac{\partial \bar{\mathbf{u}}_h}{\partial t} + w' \frac{\partial \bar{\mathbf{u}}'}{\partial z} + f \mathbf{k} \times \bar{\mathbf{u}}_h = - \frac{\partial \bar{p}}{\partial z} \hat{\mathbf{e}}_z + \mathbf{g} \quad (\text{D.32a})$$

$$\frac{\partial \bar{p}}{\partial t} + w' \frac{\partial \bar{p}'}{\partial z} = - \frac{\partial \bar{\mathbf{J}}_{rad}}{\partial z} + \kappa \frac{\partial^2 \bar{p}}{\partial z^2} \quad (\text{D.32b})$$

where the RHS of equation (D.32a) is hydrostaticity, leaving $w' \frac{\partial \bar{w}'}{\partial z} = 0 \rightarrow \frac{\partial \bar{w}'}{\partial z} = 0$ for the vertical part, hence:

$$\frac{\partial \bar{\mathbf{u}}_h}{\partial t} + \frac{\partial w' \bar{\mathbf{u}}'_h}{\partial z} + f \mathbf{k} \times \bar{\mathbf{u}}_h = 0 \quad (\text{D.33a})$$

$$\frac{\partial \bar{p}}{\partial t} + \frac{\partial w' \bar{p}'}{\partial z} = - \frac{\partial \bar{\mathbf{J}}_{rad}}{\partial z} + \kappa \frac{\partial^2 \bar{p}}{\partial z^2} \quad (\text{D.33b})$$

$$\frac{\partial \bar{\mathbf{u}}_h}{\partial t} + \frac{\partial w' \bar{\mathbf{u}}'_h}{\partial z} + f \mathbf{k} \times \bar{\mathbf{u}}_h = 0 \quad (\text{D.34a})$$

$$\frac{\partial \bar{p}}{\partial t} = - \frac{\partial}{\partial z} \left(w' \bar{p}' - \bar{\mathbf{J}}_{rad} + \kappa \frac{\partial \bar{p}}{\partial z} \right) \quad (\text{D.34b})$$

^a $\delta_h = 1 - \delta_3$

diffusion term very small on macro scale?

Derivation 10: Turbulent Kinetic Energy

Multiplication of equation (D.28a) with u'_i over all i yields

$$\begin{aligned} & u'_i \frac{\partial(\bar{u}_i + u'_i)}{\partial t} + u'_i (\bar{u}_j + u'_j) \frac{\partial(\bar{u}_i + u'_i)}{\partial x_j} + u'_i \delta_{j3} \epsilon_{jki} f_j (\bar{u} + u')_k \\ & = - u'_i \frac{\partial(\bar{p} + p')}{\partial x_i} + u'_i \nu \frac{\partial^2(\bar{u}_i + u'_i)}{\partial x_j^2} - u'_i \delta_3 \bar{g} \end{aligned}$$

$$\begin{aligned} & \frac{1}{2} \frac{\partial u'^2}{\partial t} + \frac{1}{2} \overline{u_j} \frac{\partial u_i'^2}{\partial x_j} + u_i' \overline{u_j} \frac{\partial \overline{u_i}}{\partial x_j} + u_i' u_j' \frac{\partial \overline{u_i}}{\partial x_j} + \frac{1}{2} u_j' \frac{\partial u_i'^2}{\partial x_j} \\ & = -u_i' \frac{\partial \overline{p}}{\partial x_i} - u_i' \frac{\partial p'}{\partial x_i} + u_i' \nu \frac{\partial^2 \overline{u_i}}{\partial x_j^2} + \frac{1}{2} \nu \frac{\partial^2 u_i'^2}{\partial x_j^2} - \nu \left(\frac{\partial u_i'}{\partial x_j} \right)^2 - u_i' \delta_{3g} \end{aligned} \quad (\text{D.35})$$

First and last term on RHS are again hydrostaticity

$$\begin{aligned} & \frac{1}{2} \frac{\partial u'^2}{\partial t} + \frac{1}{2} \overline{u_j} \frac{\partial u_i'^2}{\partial x_j} + u_i' \overline{u_j} \frac{\partial \overline{u_i}}{\partial x_j} + u_i' u_j' \frac{\partial \overline{u_i}}{\partial x_j} + \frac{1}{2} u_j' \frac{\partial u_i'^2}{\partial x_j} \\ & = -u_i' \frac{\partial p'}{\partial x_i} + u_i' \nu \frac{\partial^2 \overline{u_i}}{\partial x_j^2} + \frac{1}{2} \nu \frac{\partial^2 u_i'^2}{\partial x_j^2} - \nu \left(\frac{\partial u_i'}{\partial x_j} \right)^2 \end{aligned} \quad (\text{D.36})$$

averaging...

$$\frac{\partial E_t}{\partial t} + \overline{u_j} \frac{\partial E_t}{\partial x_j} - \nu \frac{\partial^2 E_t}{\partial x_j^2} = -\overline{u_i' \overline{u_j} \frac{\partial \overline{u_i}}{\partial x_j}} - \overline{u_i' u_j' \frac{\partial \overline{u_i}}{\partial x_j}} - \frac{1}{2} \overline{u_j' \frac{\partial u_i'^2}{\partial x_j}} - \overline{u_i' \frac{\partial p'}{\partial x_i}} + \nu \overline{u_i' \frac{\partial^2 \overline{u_i}}{\partial x_j^2}} - \nu \left(\overline{\frac{\partial u_i'}{\partial x_j}} \right)^2 \quad (\text{D.37})$$

...

$$\frac{\partial E_t}{\partial t} + \overline{u_j} \frac{\partial E_t}{\partial x_j} = \frac{\partial}{\partial x_j} \left(\nu \frac{\partial E_t}{\partial x_j} + \overline{u_j' p'} + \frac{1}{2} \overline{u_j' u_i' u_i'} \right) - \overline{u_j' u_i' \frac{\partial \overline{u_i}}{\partial x_j}} + \overline{b' w'} - \nu \left(\overline{\frac{\partial u_i'}{\partial x_j}} \right)^2 \quad (\text{D.38})$$

$$\frac{\partial E_t}{\partial t} + \overline{u_j} \frac{\partial E_t}{\partial x_j} = \frac{\partial \psi}{\partial x_j} - \overline{u_j' u_i' \frac{\partial \overline{u_i}}{\partial x_j}} + \overline{b' w'} - \nu \left(\overline{\frac{\partial u_i'}{\partial x_j}} \right)^2 \quad (\text{D.39})$$

... with $\psi = \nu \nabla E_t + \overline{\mathbf{u}' p'} + \frac{1}{2} \overline{\mathbf{u}' \mathbf{u}''^2}$ as the total flux of turbulent kinetic energy.

Invoking again horizontal homogeneity as was done for equation (D.32a), equation (D.39) takes the form

$$\frac{\partial E_t}{\partial t} + \overline{w} \frac{\partial E_t}{\partial z} = \frac{\partial \psi}{\partial z} - \overline{\mathbf{u}_h' w' \frac{\partial \overline{\mathbf{u}_h}}{\partial z}} + \overline{b' w'} - \nu \overline{(\nabla \mathbf{u}')^2} \quad (\text{D.40})$$

derivation still incomplete.. i
assume $\overline{ab'} = \overline{ab}$
might help..?

Appendix E

Preview...

just a couple of graphics i had laying around...

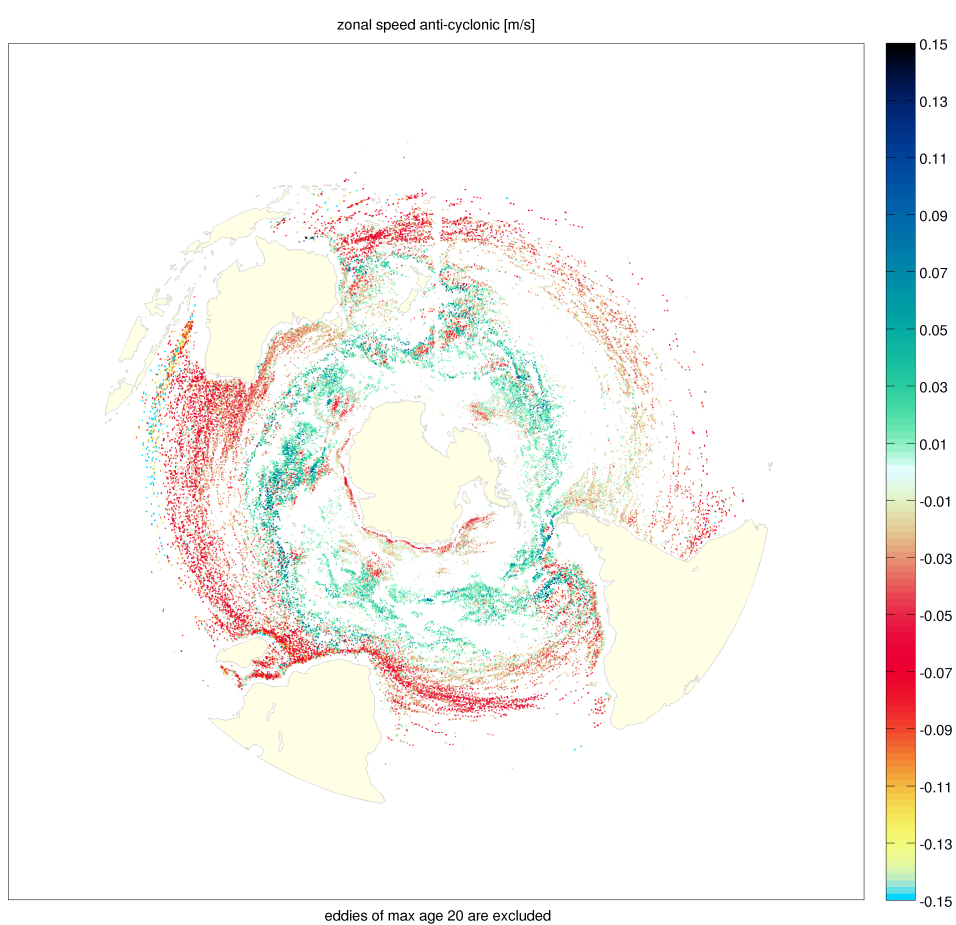


Figure E.1: ACC drift speeds

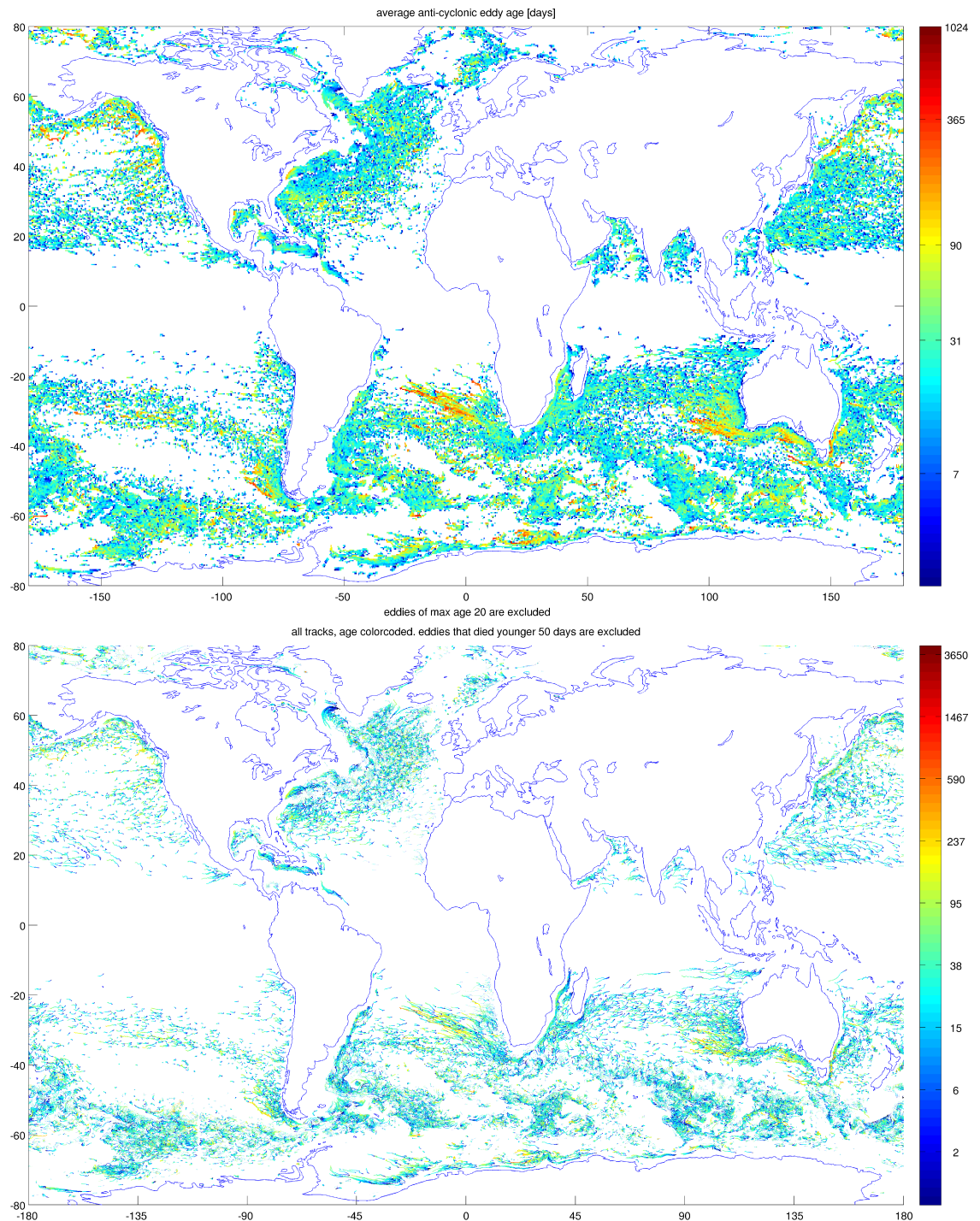
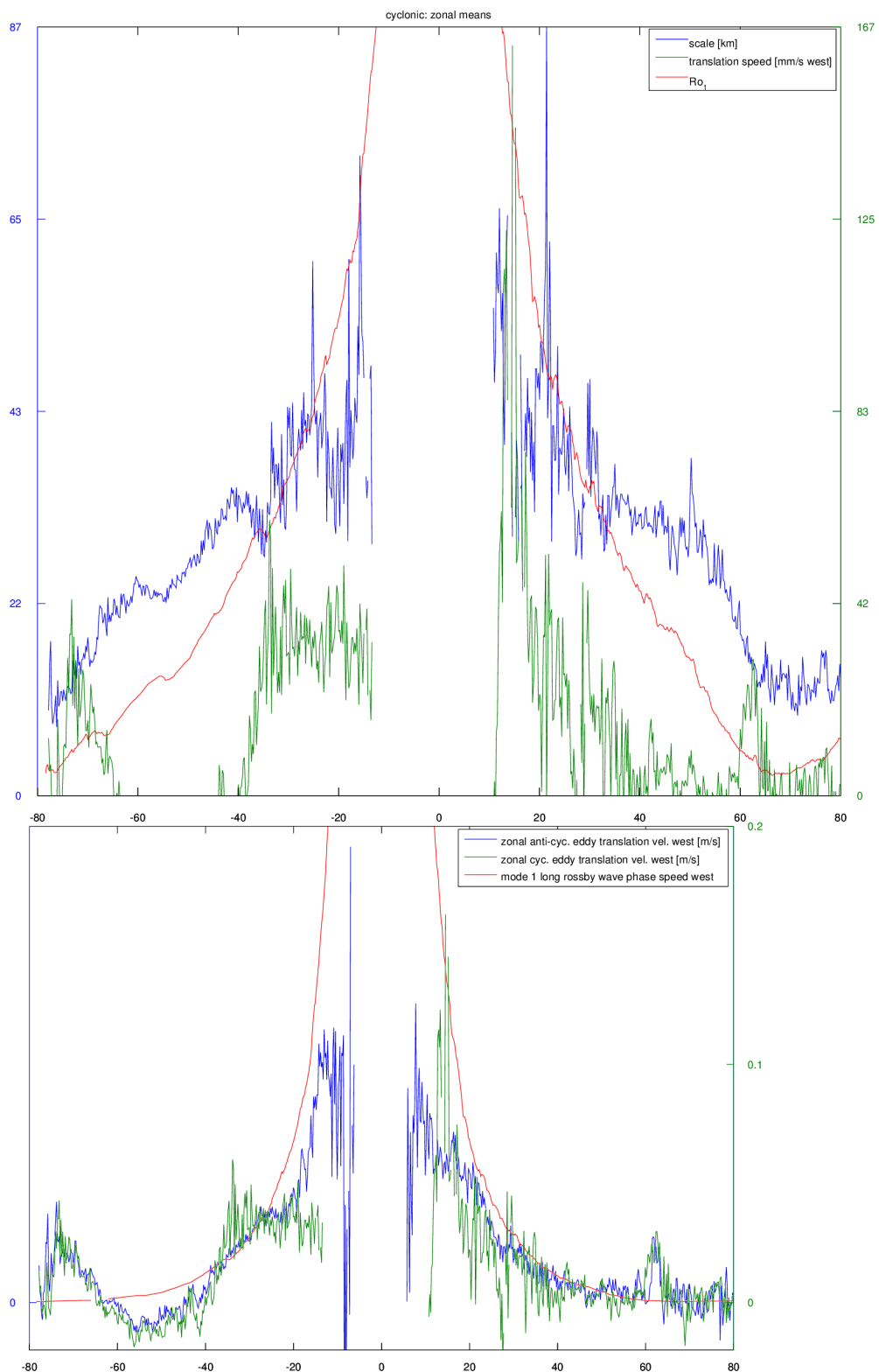


Figure E.2: note: scales are wrong! shifted by 20 respective 50 days...



Declaration of Authorship

I, Nikolaus KOOPMANN, declare that this thesis titled, 'Automated Analysis of Meso-Scale Ocean-Eddies from Model Data' and the work presented in it are my own. I confirm that:

- This work was done wholly or mainly while in candidature for a research degree at this University.
- Where any part of this thesis has previously been submitted for a degree or any other qualification at this University or any other institution, this has been clearly stated.
- Where I have consulted the published work of others, this is always clearly attributed.
- Where I have quoted from the work of others, the source is always given. With the exception of such quotations, this thesis is entirely my own work.
- I have acknowledged all main sources of help.
- Where the thesis is based on work done by myself jointly with others, I have made clear exactly what was done by others and what I have contributed myself.

Signed: _____

Date: _____

Acknowledgements

The acknowledgements and the people to thank go here, don't forget to include your project advisor...

Todo list

■ abstract	iii
■ vector based detection etc	2
■ ref to technical chapter	4
■ ? for derivation if time	5
■ ref	5
■ rephrase	6
■ ref to section	8
■ ref	11
■ TODO!	12
■ compare both, show pictures	14
■ theres probably a better way via okubo weiss!	14
■ show map	16
■ U.path.TempSalt.name='TempSalt';	16
■ explain	17
■ plots to follow...	17
■ results...	19
■ discussion...	21
■ solve for h instead of rho in mass budget	29
■ reminiscent of QPVE, try again later..	29
■ maybe show derivation from vallis...	30
■ ref to here later - argument for further tracking depth	30
■ diffusion term very small on macro scale?	37
■ derivation still incomplete.. i assume $\bar{ab}' = \bar{a}\bar{b}$ might help..?	38